To the Graduate Council:

I am submitting herewith a thesis written by Nathaniel Kennedy entitled "The Improvement of Wear Characteristics of Aluminum Through the Addition of Silicon Via Laser Processing." I have examined the final copy of this thesis for form and content and recommend that it be accepted in partial fulfillment of the requirements for the degree of Master of Science, with a major in Engineering Science.

John Hopkins, Major Professor

We have read this thesis
and recommend its acceptance:

Accepted for the Council:

Associate Vice Chancellor and
Dean of The Graduate School

THE IMPROVEMENT OF WEAR CHARACTERISTICS OF ALUMINUM THROUGH THE ADDITION OF SILICON VIA LASER PROCESSING

A Thesis
Presented for the
Master of Science
Degree
The University of Tennessee, Knoxville

Nathaniel Kennedy
May 1999

DEDICATION

This thesis is dedicated to God
for giving me the ability, and to my
parents for giving me the opportunity.

ACKNOWLEDGMENTS

I owe a great deal to several people without whom this thesis surely would have never been completed.

I would first like to thank my professors here at the Space Institute. As my major professor Dr. John Hopkins provided friendship, insight, and guidance. His help has been invaluable to me. I would also like to thank Dr. Mary Helen McCay for the example she set for me, as a researcher, a teacher and a leader.

I would also like to thank those people who I worked with on a daily basis. To Brent Blaha, Jacob Cashion, Ivan Dors, and Dean Ferrell for making my time at CLA enjoyable. Credit is also due to those men outside of CLA who provided me with refuge: Joe Hane, Ricky Meeker, and Gary Payne. Thanks to all of you for the friends you have been.

I owe a great deal to my family for helping and encouraging me to this end. Thank you.

To Glen Tyree, Jason Klepper, and Scott Sowles thanks for always letting me know I had friends I could turn to.

Finally, to Rachel for sticking with me through two years apart, for lending encouragement and support and for your love.

ABSTRACT

Engine weight reduction is a primary concern to automotive manufacturers regardless of the size of the vehicle. Engine blocks made from aluminum reduce weight, but result in excess engine wear. One possible solution is Laser Induced Surface Improvement (LISI) applied directly to the cylinder wall. It was hypothesized that through the LISI process a aluminum-silicon hypereutectic alloy could be created with significant improvements in wear resistance over unprocessed aluminum. Here an attempt has been made to investigate, through a series of tests, the optimal silicon content for improvement of wear characteristics of aluminum A319. Flat coupon trials were conducted using various processing conditions and precursor compositions. Performance was evaluated and ranked through metallurgical analysis and bench wear testing. Once an optimal precursor was chosen, limited duration testing was conducted on a 13 cubic inch aluminum air-cooled single cylinder to demonstrate performance in an engine environment and compare to parent bore test results. Through this study, it was shown that LISI is a viable option for producing wear resistant surfaces on aluminum cylinder bores.

TABLE OF CONTENTS

CHAPTER	PAGE
1 INTRODUCTION	1
2 BACKGROUND	5
1 Wear Problems within Internal Combustion Engine	5
2 Proposed Solutions	7
3 Wear in Aluminum-Silicon Alloys	12
4 Theories on Wear	17
5 Laser Alloying	19
3 EXPERIMENTAL PROCEDURE	21
1 Choice of Matrix	21
2 Sample Preparation	23
3 Laser Processing and Post Laser Processing Analysis	24
4 Second Set of Samples	26
5 Engine Processing	27
4 EXPERIMENTAL APPARATUS	28
1 Processing Apparati	28
1.1 Spray Booth	28
1.2 Laser	28
2 Analysis Apparati	31
2.1 Lubricated Sliding Wear Tester	31
2.2 Dry Sliding Wear Tester	33
2.3 Microhardness Tester	33
2.4 Digital Imaging	33
2.5 Scanning Electron Microscope	34
3 Engine Testing	34
5 RESULTS AND DISCUSSION	36
1 Layer Depths	36
2 Silicon Content for RDY 744	40
3 Silicon Content for RDY 836	45
4 SEM Results for Eight Samples	48
5 Copper and Magnesium Compositions	52
6 Hardness Results	55
7 Dry Wear Results	55
8 Lubricated Wear Results	64
9 Final Composition	64
10 Engine Bore Results	67
11 Sources of Error	71
6 CONCLUSIONS	72
1 Results	72
2 Future Work	73
BIBLIOGRAPHY	62
VITA	66

LIST OF TABLES

TABLE		PAGE
1	Summary of Wear Resistance Research on Aluminum-Silicon Alloys	14
2	Processing Conditions	25
3	RDY 744 Layer Depths with Conditions and Rankings	39
4	RDY 836 Processing Conditions and Layer Depth	41
5	Silicon Content of RDY 744 Samples	44
6	Silicon Content of RDY 836 Samples and Layer Depth	46
7	Silicon Content Comparison of RDY 744 and RDY 836	46
8	Comparison of Silicon Content Between Four Point Analysis and Compositional Map	49
9	Silicon Content at Three Different Locations in the Layer	50
10	Copper and Magnesium Compositions	54
11	Hardness Values of Laser Processed Samples	54
12	Results from Dry Wear Tests	59
13	Temperature Measurements Recorded During Dry Wear Testing	59
14	Silicon Content and Volumetric Wear Loss of Laser Processed Samples	63
15	Lubricated Wear Test Results	65

LIST OF FIGURES

FIGURE		PAGE
1	Schematic Diagram of LISI	3
2	Aluminum-Silicon Phase Diagram	13
3	Spray Booth	29
4	Laser Setup Before Processing Engine Block	30
5	Lubricated Wear Tester	32
6	Engine on Dynamometer	35
7	Cross Section of Unprocessed Aluminum 319 Showing Inherent Porosity	37
8	Cross Section of RDY 7445-2	38
9	Layer Depth as a Function of Laser Beam Speed	42
10	Layer Depth as a Function of P/V for RDY 744	43
11	Layer Depth as a Function of P/V for RDY 836	47
12	Silicon Content Distributed Through the Layer	51
13	X-Ray Compositional Map of RDY 836-1	53
14	Hardness as a Function of Silicon Content	56
15	RDY 7445-2 at 2000 X	57
16	RDY 836-2 at 200 X	58
17	Volumetric Dry Wear Loss Comparison of Laser Processed Samples	60
18	Dry Wear temperature Measurements After Two Minutes of Testing	62
19	Lubricated Wear Comparison Between Iron, Aluminum and Laser Processed Samples	66
20	Closeup of Cylinder Wall of Block #1 After Processing	68
21	Closeup of Cylinder Wall of Block #2 After Processing	69
22	Wear Measurements of Control and LISI Engine	70

NOMENCLATURE

q	rate of wear
W	applied load
R_c	Rockwell hardness on c-scale
τ	beam interaction time
P/V	laser power divided by laser velocity

Abbreviations

EDS	energy dispersive spectroscopy
HVOF	high velocity oxygen fuel
ICE	internal combustion engine
LISI	laser induced surface improvements
MMC	metal matrix composites
RDY	research and development YAG
RPM	revolutions per minute
SAE	society of automotive engineers
SEM	scanning electron microscope
YAG	yttrium aluminum garnet

CHAPTER 1

INTRODUCTION

Engine blocks made of aluminum offer many advantages over their iron counterparts including reduced emissions and improved fuel economy. The weight difference between iron and aluminum is the key factor with aluminum roughly 2.5 times lighter than iron by volume. Reduced emissions and improved fuel economy are two goals achieved through weight reduction. However, aluminum is limited by the fact that it does not resist wear as well as iron. Since wear resistance is especially critical within the cylinder bore it has left automotive manufacturers searching for an engine block that has the low weight of aluminum and the wear characteristics of iron.

A number of alternatives have been explored by automobile manufacturers in an attempt to solve this problem. The most common approach has been to cast or press iron liners into the aluminum block. Not only does this significantly increase the block's weight and reduce the engine's displacement, but it also requires additional manufacturing steps.

Nikasil™ is a plating process that has been used in aluminum blocks in the motorcycle industry for many years. However, there are a several limitations that keep this from becoming an effective option for high production automotive engines. Another proposed solution is to make the blocks out of Metal Matrix Composites (MMC). MMCs have been examined extensively by Honda Motor Corporation with mixed results (Bell, 1997).

Two techniques that have received increased attention from the automotive industry in the last few years due to improved technology are High Velocity Oxygen Fuel (HVOF) and Plasma-sprays (Irving, 1998). HVOF spray is a process by which an oxygen torch is used as a supersonic gas jet to deposit small molten metallic or ceramic particles onto a substrate. The layer can be built up by making multiple passes with the torch. This technology is currently under development (Irving, 1998). Plasma-spray is similar to HVOF, but instead of using a high velocity torch, the combination of an electric arc and low velocity plasma gas is used to propel molten particles onto the target.

Another approach has been to make the entire block from a hypereutectic material. Mercedes recently introduced a new aluminum V-6 engine that uses cylinder liners made from a material called Silitec. Silitec is a specially cast aluminum alloy that contains 18 weight percent silicon, 4 percent weight copper and 1 weight percent magnesium.

A proposed solution to this problem is Laser Induced Surface Improvement (LISI). LISI is a two-step process, by which a precursor material is first applied to the cylinder bore, allowed to dry, and then processed with a laser beam [Figure 1]. The precursor is comprised of a mixture of metallic powder and commercially available liquid binder for spraying. First, the precursor is sprayed on the cylinder walls and allowed to dry. The substrate and the precursor are then alloyed together using a laser beam. The laser beam melts both the precursor and a portion of the substrate and the precursor together through convection followed by rapid (10^6 C s^{-1})

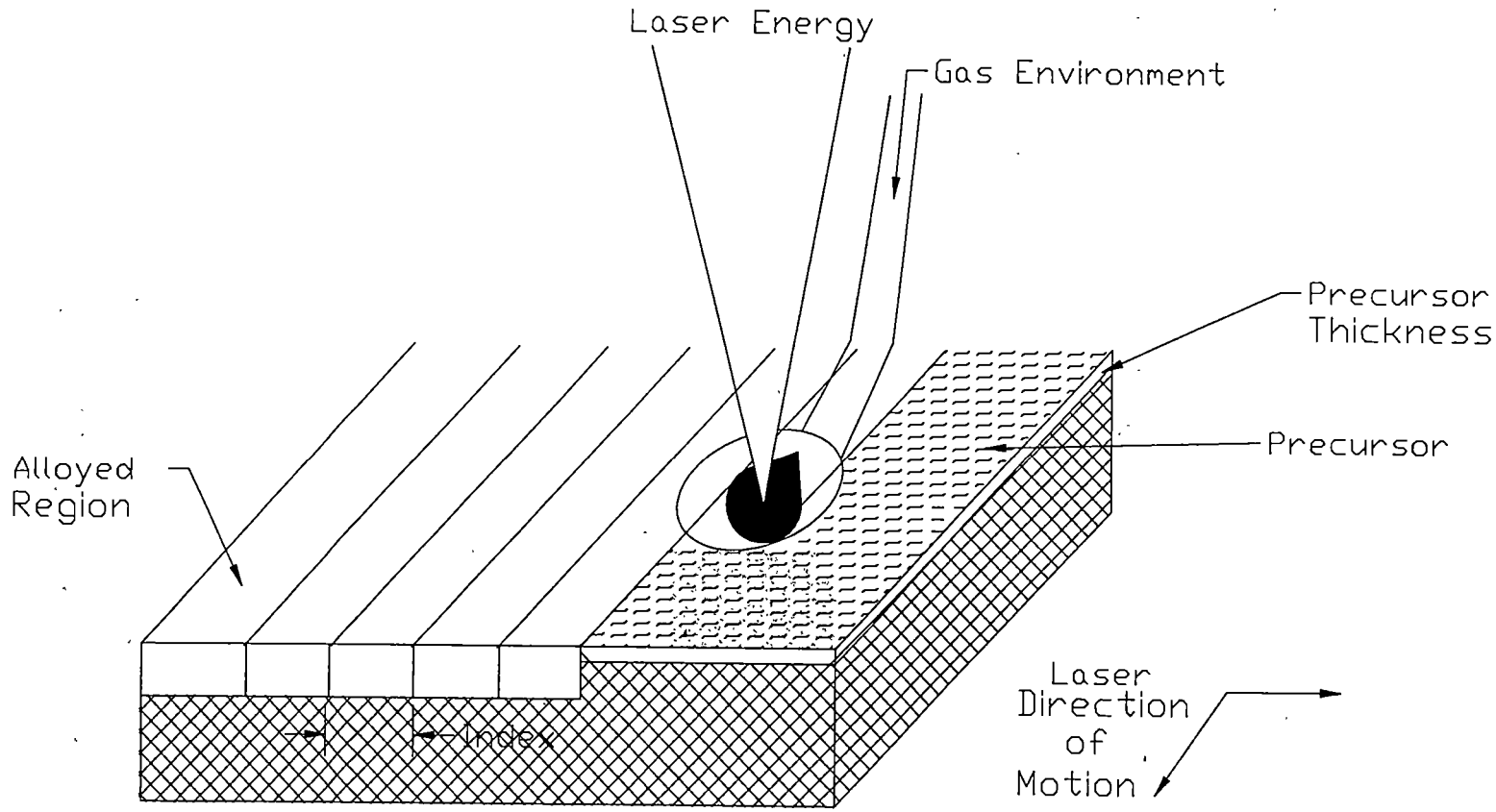


Figure 1: Schematic Diagram of LISI

cooling and solidification. In the present case, the metallic powder is a silicon-copper-aluminum combination. The materials are added to the aluminum substrate with the intent of improving the wear properties of the parent bore surface.

CHAPTER 2

BACKGROUND

This chapter examines the need for enhancing wear resistance within the cylinder bore, some proposed solutions, a background of aluminum-silicon alloys and the nature of their wear.

2.1 Wear Problems within Internal Combustion Engine

Within an internal combustion engine (ICE), there are certain wear problems that must be addressed. The most prominent of these is the wear that occurs within the cylinder bore between the piston/ piston rings and the wall of the cylinder. It is difficult to use an aluminum piston with an aluminum bore. During periods of low lubrication, such as cold starts, the two aluminum surfaces adhere to each other and scuffing may occur (Qui, 1996).

The operating environment within a cylinder bore is unique. In automotive engines, the system must be able to run millions of cycles at with peak combustion temperatures above 3000 degrees Celsius without failure (Stone, '92). A delicate balance exists between the piston rings and the cylinder walls. The rings must be close enough to the wall to maintain hydrodynamic lubrication and insure there is no blow-by but at the same time not be so close as to result in excessive wear.

Abrasion from hard particles in the oil film tends to be the most common source of wear on both the piston rings and cylinder bore. These hard particles can result as a product of the wear itself or from within the combustion zone. The

abrasion is most evident at top dead center on the cylinder bore (Eyre, 1990). During both the compression and expansion strokes, the top ring twists due to high gas pressure and large clearance. This allows the upper edge of the ring to make contact with the cylinder wall creating maximum wear (Hofmann, 1983).

The face-centered cubic structure of aluminum contains four {1 1 1} planes and three <1 1 0> directions of densely populated atoms thereby providing twelve slip systems. These densely packed atoms help to promote easy slip and plastic deformation. According to Davis and Eyre (1994), there are two mechanisms by which the addition of silicon helps an aluminum alloy during sliding wear. By adding a nonmetallic, such as silicon, the metallic wear is limited to just the aluminum fraction. Also, the presence of silicon helps to raise the yield strength of the alloy enabling it to better support an oxide film. Using this reasoning, it can be seen that increased silicon content, should improve wear resistance (Davis, 1994).

One other problem with traditional hypereutectic aluminum engine blocks is the need for iron coated pistons. This is because of the poor sliding wear between two aluminum surfaces, especially during periods of low lubrication, such as cold starts. When two hypereutectic aluminum-silicon alloys are exposed to each other under wear conditions such as those that occur in an engine, the primary silicon particles in one material contact and attempt to dislodge the primary silicon in the other surface. This results in "pull-out" damage and sub-surface cracking (Donahue, 1993).

2.2 Proposed Solutions

The automotive industry has invested large sums of both time and money in an effort to solve the problem of excessive wear in aluminum blocks. The most common approach is to make the block out of aluminum, and then use cast iron liners. These liners can be designed to be either wet or dry sleeve. There are several problems with this solution besides the increased weight and loss of displacement. The iron liners also offset the heat transfer advantages of the aluminum and as previously mentioned, the number of production steps are increased because the block must be honed twice. As the number of production steps increases, so does the cost of production.

The first widely used hypereutectic aluminum engine was made from the 390 alloy developed by Reynolds Metals Company for General Motors. A390 Al is a hypereutectic aluminum alloy that contains between 16.0-18.0 weight percent silicon, 4.0-5.0 weight percent copper and 0.45-0.65 weight percent magnesium along with other trace elements (ASM, 1979). It was first used in the Chevrolet Vega in the early 1970's. This engine was deemed to be a failure for reasons other that than the bore technology. However, GM felt that public confidence in the engine was too poor to overcome and the project was dropped. At the same time the A390 Al alloy was used in Corvette ZL-1 racing engines with a great deal of success. This lead to the development of several Porsche racing engines made from the alloy. Ultimately, Porsche manufactured three A390 Al engines for use in both the 928 and 944 models. Mercedes, Audi and BMW also found successful applications for the A390 Al

engines (Jorstad, 1996). Due to the fact that the A390 Al alloy is hypereutectic, production creates tooling and machining costs as well as complex castings that are prohibitively expensive for high-production models.

One solution to the problem of excess wear within aluminum engines that has been used for many years in the motorcycle industry and high performance, low production automotive market is electro-plating. The most common plating process for cylinder bores is Nikasil™ a process developed by Mahle. Nikasil™ is a deposited, via electro-plating, 80-micron thick coating of nickel dispersed with very small (1-3 microns) silicon carbide particles on the engine bore. The surface can then be honed to less than a three-micron surface roughness (Scarlett, 1996). Porsche, Ferrari, Jaguar and BMW are a few of the automobile companies who have used Nikasil™ plated cylinder bores. Jaguar claims that an eight cylinder engine plated with Nikasil™ is up to 15 pounds lighter than one using cylinder liners (Scarlett, 1996). The process has been in existence for a number of years as companies have perfected it. However, there are a number of drawbacks including increasingly stringent environmental regulations on plating processes (Hopkins, McCay, 1998). Another problem, as with any plating process, is the possibility of delamination.

Some manufacturers have also had problems using Nikasil™ plated engines in the U.S. due to the high sulfur content in U.S. fuels (Bretta, 1998). BMW ran into this problem with the V-8 engines in their cars from 1993-1995. As the sulfur attacked the Nikasil™ on the cylinder wall, the piston rings were no longer able to seat properly resulting in "leakdown" or "blow-by." This problem eventually resulted

in BMW doubling its warranty to 100,000 miles and replacing the entire shortblock with blocks made entirely from Alusil™, a brand of hypereutectic aluminum-silicon alloy (Bretta, 1998).

Another option, explored thoroughly by Honda Motor Corporation, has been to develop an engine block made from MMCs. They have been used in the Honda Prelude 2.2L DOHC I-4 engine (Cole, 1993). These blocks are made from aluminum matrix composites reinforced with carbon fibers. The carbon fibers serve two purposes: Firstly, they help improve the sliding characteristics within the cylinder bore, and secondly they add strength to the block (Imura, 1992). While the added strength helps reduce wear within the cylinder, it does lead to increased tooling wear. Due to inadequate tooling technology, machining is often a trial and error process, making production difficult (Bell, 1997). Honda eventually resorted to sintered diamond chips to bore out the cylinder, dramatically increasing tooling costs (Imura, 1992).

One approach that would be categorized as an MMC is Lokasil™. This process was developed by, Kolbenschmidt, a German company. They use a silicon-imbedded ceramic preform in the vicinity of the cylinder bore that is then squeeze cast and filled with molten alloy. This yields bore surfaces similar to A390 Al, but with better casting and machinability throughout the rest of the block (Jorstad, 1996).

Another manufacturing alternative currently under development is plasma-spray. There are several different types of plasma sprays currently under investigation. The two most promising processes are Plasma Transfer Wire Arc and Plasma Powder spray process (Rao, 1997). The wire arc method offers simplicity and

ease of implementation in a production line. The powder spray process is receiving new attention due to the invention of a new automatic rotating plasma-spray gun that coats the bore with metal encapsulated solid lubricants (Rao, 1997). In this case, the metal is a molybdenum-based alloy (Irving, 1998). Both methods are currently being researched at Ford Motor Corporation (Rao, 1997).

Another technique, which falls under the category of thermal sprays, is HVOF technology. In the HVOF process, liquid fuel and oxygen are fed into a combustion chamber at high pressures where they burn to produce a hot gas stream. This is expanded through a nozzle, at which point the powder is injected into the stream. The powder is not necessarily melted, but may only be softened as it is brought to a temperature near the melting point and shot onto the substrate at a speed of over 1500 m/sec (Irving, 1998).

The major drawback with HVOF and plasma sprays, is the same as Nikasil™: they are merely coatings and the coating eventually wears off leaving the parent bore exposed. There is also a concern with spraying too much material on the surface. Surface preparation has proven to be a critical issue with these techniques. The surface must be degreased and have an adequate surface roughness in order for the coating to adhere properly. More recently, plasma-spray technology has reached the level where a surface flux is used in lieu of preparing the surface. Noise is also considered a major concern during spraying for these processes.

Mercedes-Benz has developed a solution using cylinder sleeves made from a low-friction hypereutectic alloy called Silitec™. Silitec™ contains 18 weight percent silicon, 4 weight percent copper and 1 weight percent magnesium. The use of

cylinder liners made from Silitec™ cuts piston-ring spring tension in half (Advanced Materials, 1997). The sleeves also help to provide more block stiffness while keeping weight to a minimum. The Silitec™ sleeves are more than a pound lighter than identical sleeves made from iron. The combination of an all-aluminum block and the Silitec™ sleeves results in a total block weight of only 57 pounds (Advanced Materials, 1997). However, the use of cylinder liners still leads to reduced displacement within the bore and an increase in production steps.

Cylinder liners similar to Silitec™ can be made using a method invented by Donahue et al. This process involves feeding hypereutectic molten alloy into a metal mold with an inner sand shell while the rotating the mold at 1000 rpm. The purpose of spinning the mold is to allow centrifugal force to create an inward migration of silicon particles. The sand shell provides insulation, thus elongating the fluid life of the alloy. This results in a higher volume fraction of silicon particles near the wear surface. This process allows a liner to be produced with the wear properties of an alloy of much higher silicon content, but with the castability of a lower silicon alloy (Donahue, 1994).

Laser surface modifications offer many advantages over other techniques. The possibility of delamination that is encountered with Nikasil™, HVOF and Plasma-sprays is eliminated with LISI because the substrate and the precursor are alloyed together. Unlike plating processes, LISI has no by-products making it environmentally friendly. Where HVOF uses jets to blast metallic particles at supersonic speeds, the LISI process uses a laser, making LISI a much quieter process.

One of the main problems in the search for solutions to excessive cylinder bore wear within an aluminum engine is that the ideal surface has yet to be defined. However, LISI offers greater flexibility once the ideal surface is determined. Layers formed through laser processing are anywhere from 5-30 times thicker than typical plated surface treatments (Volz, 1997). It is possible for LISI to yield alloyed regions up to 1 mm deep, allowing for extended wear resistance within the cylinder bore. However, it is also possible to use LISI for small material additions. If it was determined the entire cylinder did not need processing, LISI offers the advantage of being able to process selected regions within the bore.

2.3 Wear in Aluminum-Silicon Alloys

Aluminum-silicon alloys have been investigated for a number of years [Table 1]. The eutectic point of a binary aluminum-silicon alloy occurs at the point where the lowest melting point occurs. As can be seen from the phase diagram, [Figure 2] the eutectic point of aluminum-silicon is at 12.5 percent silicon and 577°C. Alloys with silicon content larger than 12.5 percent are known as hypereutectic.

The wear characteristics of hypereutectic aluminum-silicon alloys have been investigated for over 30 years with varying results. Okabayashi et al. first investigated silicon content in aluminum-silicon alloys in 1966. They concluded that wear resistance improved as the silicon content increased. In 1968, Vandelli tested wear on samples with 14.5, 17 and 25 percent Si. Vandelli concluded, contrary to

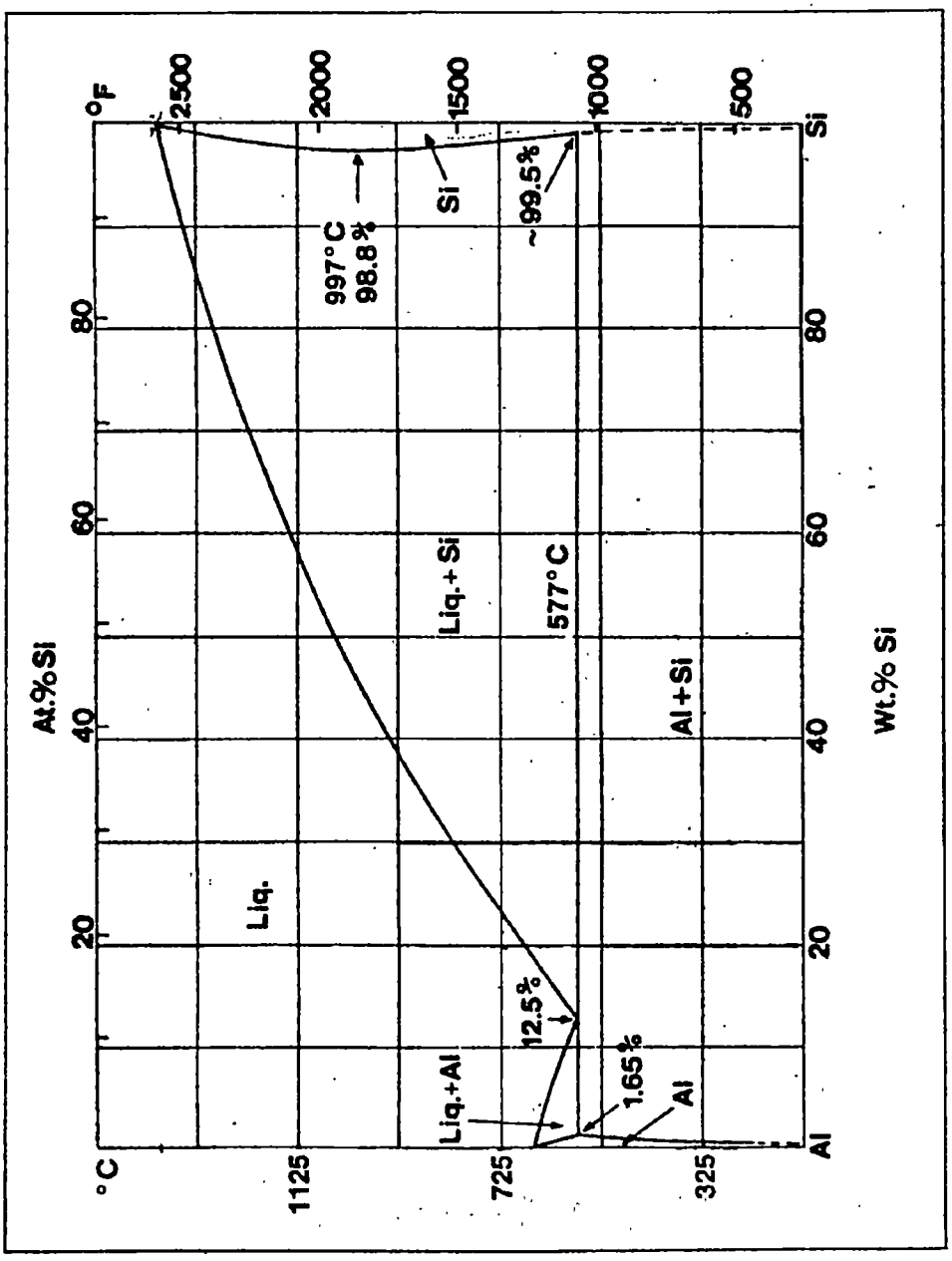


Figure 2: Aluminum-Silicon Phase Diagram.

Tables 1: Summary of Wear Resistance Research on Aluminum-Silicon Alloys.

Publisher	Year	Conclusions
Okabayashi	1966	Sliding wear resistance improves with increased silicon content.
Vandelli	1968	Best sliding wear performance occurs at 17 percent silicon.
Okabayashi	1968	Best sliding wear performance occurs at 21.6 percent silicon content. Amount of primary silicon is far more important than particle size.
Sarkar	1975	Hypoeuctectic alloys offer better sliding wear resistance than hypereutectic.
Clark and Sarkar	1979	Best sliding wear performance occurs at 18 percent silicon content.
Andrews	1985	Sliding wear rates decrease sharply as the primary silicon content increases.
Davis and Eyre	1994	Higher silicon content yields higher loads and improves running-in wear.
Biswas and Reddy	1995	No trend in sliding wear performance for alloys between 4-24 percent silicon.

Okayabashi's work that the best wear resistance occurred at 17 percent Si. However, he concluded that wear resistance is governed more by the distribution of the silicon particles along with the amount. (Vandelli, 1968).

Also in 1968, Okayabashi and Kawamoto published results on studies they had done on 8.4, 11.7, 15.0 and 21.6 percent silicon alloys. They reported that all of the samples except the 21.6 percent had the "tendency to cause seizure at relatively high sliding speed." Their results showed similar wear for the first three samples, but a lower wear rate for the 21.6 percent sample (Okayabashi, 1968). Biswas and Reddy reported in 1995 that "there is no systematic trend in the wear of alloys containing 4-24 weight percent silicon with respect to silicon content" (Biswas, 1995).

While the majority of research points to hypereutectic alloys as superior in wear resistance, not all studies agree. In 1975, Sarkar measured the wear of two alloys, one hypoeutectic and one hypereutectic, using a pin-on-bush wear test. The bushes were made of gray cast iron. He concluded that the hypereutectic alloy wears more than the hypoeutectic. However, in 1979, Clark and Sarkar studied binary aluminum alloys with 2 to 21 weight percent silicon. Their results were similar to Vandelli's in that the intermediate silicon content showed the least wear.

In 1985, Andrews et al performed pin-on-disk wear tests on hypereutectic aluminum-silicon alloys containing 17, 20, 23 and 26 percent silicon. This gave a range in volume fraction of the primary silicon of 7-17 percent. They found the wear rates decreased sharply as the primary silicon content increased (Andrews, 1985).

One aspect of wear performance related to silicon content is the amount and size of the primary silicon particles. Davis and Eyre (1994) concluded the higher

silicon content yielded higher applied loads and improved running-in wear characteristics. They also reported that with the eleven weight percent silicon alloy, the finer the particles, the better the wear. Okayabashi and Kawamoto (1968) concluded the amount of primary silicon is far more important factor in wear performance than the size of the particles.

In cast aluminum, the primary silicon particles are larger than other particles. For use in automotive cylinders, wear resistance is improved by refining the primary silicon particles (Walker, 1986). The addition of phosphorous helps to distribute the primary silicon particles more evenly throughout the aluminum matrix. It also helps to reduce the size of the primary silicon particles, usually below 35 microns, making the hypereutectic aluminum-silicon alloy plausible for wear conditions (Donahue, 1993). When dealing with laser surface modifications, the refinement of primary silicon particles occurs naturally through rapid solidification (Walker, 1986).

Andrews et al showed that one reason large particles result in poor wear performance is because they tend to break up close to the wear surface. Metallographic examination of wear tests on a aluminum-silicon alloy with 20 percent silicon showed primary silicon particles as large as 25 μm far away from the surface. However, in the region adjacent to the wear surface, the silicon particles were only 1 μm in diameter and the surface was "highly deformed." This led them to conclude that the large silicon particles break up close to the wear surface resulting in poor wear (Andrews, 1985).

Obviously, there is a great deal of disagreement among researchers concerning the effect that silicon content has on the wear of aluminum. There is not

even agreement on whether hypereutectic or hypoeutectic materials wear better. This paper will not examine hypoeutectic aluminum samples, but will analyze the differences in hypereutectic aluminum samples.

2.4 Theories on Wear

Another aspect of the wear properties of aluminum-silicon alloys is the collection of theories as to how wear occurs. Suh first proposed his theory of delamination in 1977. This theory states that deformation occurring below the surface leads to crack nucleation and propagation parallel to the wear surface. Eventually, this leads to the removal of a layer of material. Another theory involving wear mechanisms is oxidative wear, which was first proposed by Razavizadeh and Eyre in 1982.

The oxidative wear theory involves an oxidized layer formed by the heat generated through friction. As the applied load continues to press against this oxidized layer, pieces begin to chip off in the form of thin plates (Andrews, 1985). Throughout the oxidative wear, the wear is confined to the thickness of the oxide layer and thus wear rates are kept low. This process continues until the oxide film can no longer support the applied load at which point the transition to severe wear occurs (Davis, 1994). This theory has been contested by Bai and Biswas. They performed X-ray diffraction on samples and consequently did not find any oxide in the debris. Antoniou and Borland have found the layer to be an ultra-fine mixture of aluminum, silicon and α-Fe particles created during the wear process. Bai and Biswas later confirmed this composition (Reddy, 1993).

The "transition load" is another aspect of wear which also must be taken into account. Shivanath has defined the transition load as the point at which severe wear first occurs. Andrews et al. found that the transition load increases as the silicon content increases. This is a generally agreed upon theory (Reddy, 1993). Andrews et al. also found the transition load to increase with the volume fraction of primary Si. Finally, in agreement with Suh, Andrews et al, concluded that sliding wear amongst aluminum-silicon alloys was caused by delamination (Andrews, 1985).

In Sarkar's 1975 paper, it was concluded there are two regimes of wear that take place between aluminum-silicon alloys sliding on gray iron. The first regime contains a mixture of plastic and elastic contact. It was also stated that the rate of wear, q (g/cm), is proportional to the applied load, W (g), by the equation:

$$q \propto W^{\alpha}$$

where α has a value between .40 and .60. In the second regime of wear, scuffing is found to be the result of gross plastic flow of the aluminum-silicon alloy. These proposed wear mechanisms have been confirmed in experiments by Coquerelle (1986).

It can be seen that not only do researchers differ on how silicon content affects wear, but they also disagree on the ways that wear occurs. In this paper, dry and lubricated sliding wear will be investigated. The transition loads will not be investigated as they are rarely approached within the cylinder bore environment.

2.5 Laser Alloying

Various other research projects using lasers to introduce silicon into cast aluminum have been performed. Ghosh experimented with the formation of $MoSi_2$ by laser processing on A356 aluminum for use in cylinder bores (Ghosh, 1996). In this experiment, it was found that the increase of precursor thickness from 40 to 90 μm did not improve miscibility. However, other work by Blank et al have found that load bearing capacity increases almost linearly with coating thickness (Tomlinson, 1994). Ghosh (1996) also found that the variation in power from 2200 W to 2500 W on a CO_2 laser did not significantly affect morphology or microstructure.

Other research has been performed on the addition of silicon to A319 Al by laser using LISI. Kennedy and Duncan (1997) combined silicon with Ti, Ni, Cu and Mo in three different compositions, 75 weight percent silicon, 50 weight percent silicon and 25 weight percent silicon with the remaining percentage filled in with one of the other four previously mentioned elements. Samples were processed at two speeds, 4500 and 6000 mm/min. and at constant power, 2000 W, on an Nd:Yag laser. It was found that the 75 percent silicon processed at 6000 mm/min. and the 75 percent silicon processed at 4500 mm/min. had the best average wear rates regardless of the other added element. It was also found that precursor thickness was the greatest determining factor of layer depth.

In 1983, Megaw et al. studied the effect of beam interaction time on laser cladding a silicon powder to a non heat-treatable aluminum 4.5 weight percent magnesium alloy. The beam interaction time, τ, is defined as outer beam diameter divided by the scanning speed. The tracks were created with 50kW cm^{-2} for τ=0.051,

0.061, 0.082s. At the lowest τ, there was not enough input energy for the matrix to completely encompass the silicon particles. This was not a problem at the two higher τ. The increase in τ resulted in a reduction of primary silicon particles and thus an increase in aluminum. It was also found that along with the volume fraction of primary silicon, hardness increases with increased scanning speeds while the melt depth decreases.

The purpose of this study is to investigate a series of tests for flat plate samples that eventually determine the optimal silicon content for improvement of wear characteristics. As previously mentioned, there is a great deal of disagreement amongst researchers as to which types of aluminum offer the best wear resistance. In this study, a range of silicon contents was created during flat plate trials. These samples were then examined using a SEM and tested through bench wear testing. Through the process of elimination, the matrix was reduced until a certain silicon composition was selected that was thought to offer the optimum in wear resistance. That composition was then reproduced in a small engine application for limited duration testing to compare to parent bore results.

CHAPTER 3

EXPERIMENTAL PROCEDURE

Here the procedures used to prepare the samples for processing are covered, as well as the actual processing and the sample analysis techniques.

3.1 Choice of Matrix

Cast aluminum A319 was chosen as the substrate material. This is due to its wide-spread use in cylinder bore applications (Genualdi, 1997). A390 Al has also been used as a material for engine blocks, but honing has proven difficult and costly (Cole, 1993). The specification for A319 Al calls for 5.5-6.5 weight percent silicon. This makes it a hypoeutectic aluminum. It also contains 3.0-4.0 weight percent copper and .25-.40 weight percent magnesium as well as other trace elements.

As previously stated, the purpose of this work is to add silicon to the parent aluminum through laser processing, and then determine if the addition of silicon improves the wear properties of the aluminum A319. Silicon, copper, and magnesium are the three most important elements that can be added to cast aluminum. Silicon greatly increases strength and hardness, but decreases machinability. Copper imparts strength and hardness, but it helps improve machinability. Magnesium is also added to improve strength, hardness and machinability (Genauldi, 1997). Biswas and Reddy (1995) demonstrated a material

with a 17 weight percent silicon, 5 weight percent copper and 1 weight percent magnesium had a lower coefficient of friction and performed more consistently in sliding wear tests than a sample with just 17 weight percent silicon.

The choice to study silicon compositions of 14, 18, 24, and 34 weight percents was based largely on previous work. Each of these compositions gave reason to believe that they may outperform the others. Fourteen percent is near the eutectic point, but still technically hypereutectic. Work by Biswas and Reddy (1995) suggested that a eutectic alloy (11-13 weight percent Si) would give the best results due to its reduced probability of seizure. The sample at eighteen weight percent closely resembles the composition of Mercedes-Benz's Silitec™ in relation to the silicon, copper and magnesium. A number of researchers, including Vandelli, Clark, and Sarkar have confirmed the superior wear properties of 18 weight percent silicon.

Compositions around 24 percent have been previously examined, specifically by Andrews et al. Wear tests were performed on 17, 20, 23 and 26 weight percent silicon with a range of 7-17 weight percent primary silicon. Primary silicon particles are "clumps" of pure silicon that make them larger than other silicon based particles. They found the wear rates decrease as the amount of primary silicon increases and, therefore, the 23 and 26 weight percent silicon performed best. Work performed by Biswas and Reddy (1995) suggested that the 23 weight percent silicon had a lowed seizure rate than the other samples due to a lower coefficient of friction. However, their tests were done solely on cast aluminum with the silicon added through typical casting methods and not by laser alloying.

In the current study, it was desired to determine if the effects of additional primary silicon were consistent between laser alloying and typical cast aluminum. The sample containing 35 weight percent was included to see if a large amount of silicon would affect sliding wear performance. This was due to Biswas and Reddy's (1995) report that samples with up to 24 weight percent silicon performed similarly to those at four weight percent silicon.

It was hypothesized that the 18 weight percent silicon would have the best wear results. This was based on the work done by Vandelli (1968), Clark and Sarkar (1979) and suggested by the composition of the current Mercedes cylinder liners. While no information was found to support this, it is assumed that Mercedes did some research and found the 18 weight percent to be superior as well. Contrary to Biswas and Reddy (1995), it was thought that the 14 weight percent silicon would not provide adequate wear protection because it is barely a hypereutectic material and, therefore, does not contain enough silicon. The 24 and 35 weight percent silicon were thought to contain too much primary silicon. It was theorized that the wear properties would be adversely affected due to the increase in the number of loose silicon particles leading to more abrasive wear. The processing rate and the powers were determined from previous experience. Work done by Kennedy and Duncan suggested that the chosen powers and speeds would give optimal results.

3.2 Sample Preparation

Six samples of A319 aluminum were cut into 3 inch by three inch by ¼ inch squares. Prior to spraying they were washed with water and cleaned with acetone.

They were then sprayed with varying layers of precursor. The precursor mixture was made using a combination of powder silicon, copper and aluminum. The three elements were purchased in powder form from CERAC™ Inc. Each powder had an average particle size of 25 microns. The precursor had a 3:1 silicon to copper weight ratio. The three elements were then combined with water and an organic binder material to form a consistency similar to paint. The precursor was then placed in a spray gun and applied to the substrate by use of the gun. Air was used as the carrier gas. All six samples were placed in the spray booth and sprayed simultaneously. The first sample was sprayed with one layer, the second with two layers and so on until the sixth sample was coated with six layers. The thicknesses ranged from 45 to 170 microns. The samples were then allowed to dry overnight.

3.3 Laser Processing and Post Laser Processing Analysis

Once the samples dried, they were processed with the laser beam. Four trials for each sample were conducted [Table 2]. Once processed, the samples were marked on the unprocessed side for identification purposes. At this point, the precursor thickness was measured using an optical microscope. The samples were then cut into four separate sections, one for each trial leaving a total of 24 individual samples (one from each condition). Each of the subsequently laser processed samples was then halved using a circular saw for analysis purposes. One half was mounted and polished, the other half was used for sliding wear testing.

Table 2: Processing conditions.

Power (W)	Speed (mm/min)
1750	3000
1750	4500
2000	3000
2000	4500

The mounted samples were then polished using increasingly fine sandpaper to a maximum of 800 grit. Following this, each sample was micro-polished in stages ranging from 1.0 μm to .05 μm. At this point, cross-sectional pictures were taken on an optical microscope at .75 magnification of each of the samples. Using these photographs, maximum layer depth and width were measured and recorded.

Scanning electron microscope (SEM) analysis was performed once the samples were polished. Compositional maps were taken using energy dispersive spectroscopy (EDS) technique at 4000 times magnification at four different places within the layer. Using these results, the matrix would be reduced to only those samples that met the desired compositions. By taking the average of the four semi-quantitative EDS analysis readings for each sample, the sample's silicon weight percentage was obtained. Using this average, the four samples with compositions closest to the four desired weight percentages were chosen. They were RDY 7444-2 with 14 weight percent silicon, RDY 7442-4 containing 18 weight percent silicon, RDY 7445-2 contained 24 weight percent silicon, and finally RDY 7444-4 with 37 weight percent silicon.

3.4 Second Set of Samples

In an effort to reduce the size of the original matrix, four samples were chosen to be laser processed with two speeds and two powers that were used earlier. The second set of samples were intended to duplicate RDY 7444-2, 7442-4, 7445-2, 7444-4. For every one of these samples, there were two samples of similar precursor

thickness prepared and run at identical processing parameters. This was due to the inability to measure precursor thickness until after the samples had been processed. Once processed, all of the samples underwent EDS compositional analysis. Once the silicon composition was determined, only the sample that most resembled the original was used in further testing.

3.5 Engine Processing

When the time came to process the engine block, the procedure was the same as the flat plate trials. Two blocks were sprayed with the desired precursor thickness. This was done as a matter of precaution because sometimes the casting of the material affects processing. By processing two blocks, the chances were improved that one block would be good enough to run. The precursor was allowed to dry before processing began. The blocks were processed at the same power and speed as the desired composition.

CHAPTER 4

APPARATUS

This chapter describes the major hardware apparati used in this project. These hardware are necessary to: apply the precursor to the samples, process the sample, analyze the samples, and test the engine.

4.1 Processing Apparati

4.1.1 Spray Booth

For application of the precursor to the substrate, a spray booth was used. The spray booth and the gun were both manufactured by DeVilbiss Spray Booth Products. The spray booth is fitted with a spray gun as well as a hood vent [Figure 3]. The air pressure on the gun can be varied and was set at 30 psi for these trials. Oxygen was used as the carrier gas during the spraying process. All six samples were placed together in the spray booth and sprayed simultaneously.

After spraying, the samples were allowed to dry overnight before being processed. This procedure was identical for both sets of samples.

4.1.2 Laser

A 3 kW Lumonics MW-3000 Neodymium YAG laser [Figure 4] was used to process the coupons. The beam was carried to the optics from the laser in a 600 μm diameter, 30 m long fiber optic cable. The entire beam focusing system was designed at the University of Tennessee Space Institute.

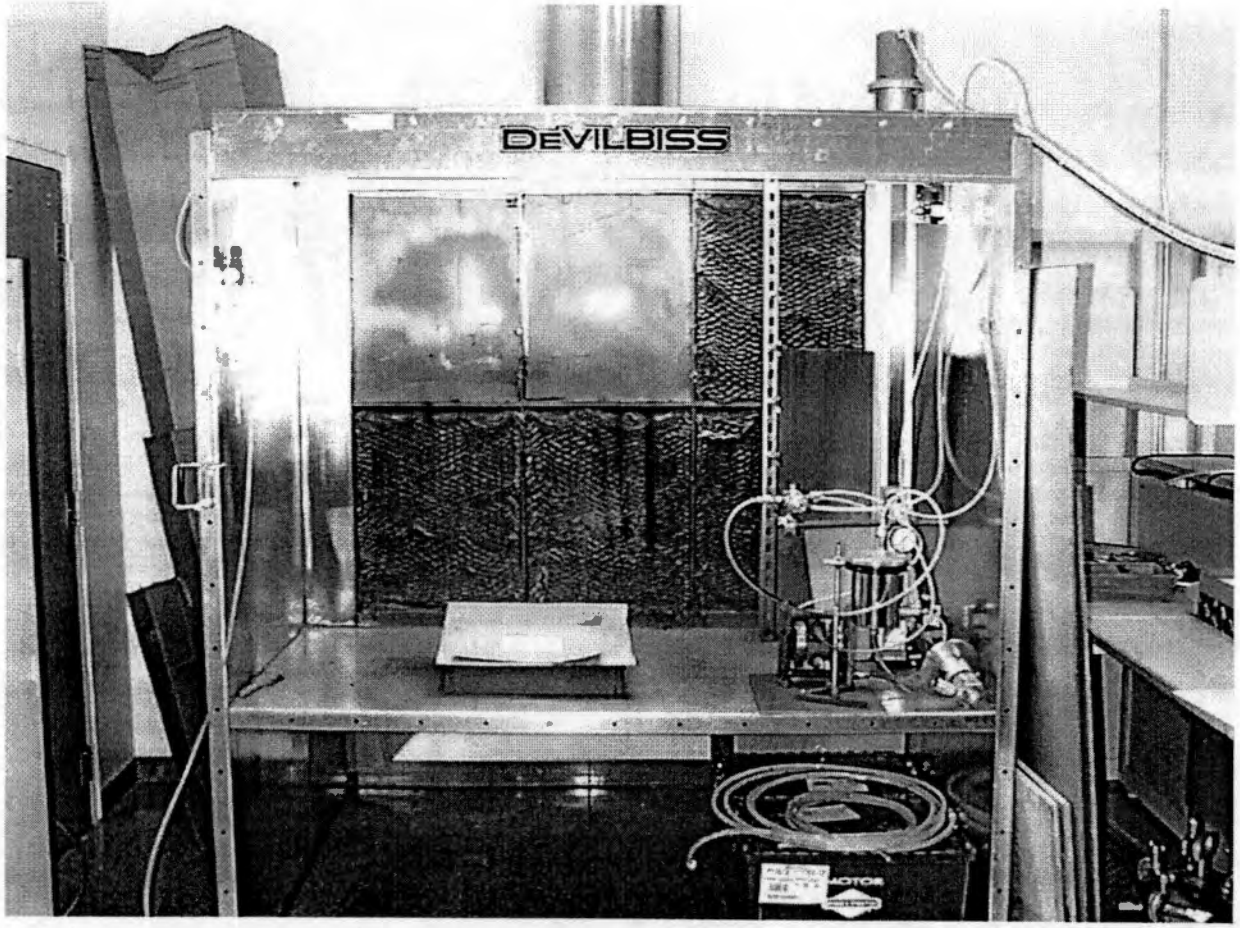


Figure 3: Spray Booth.

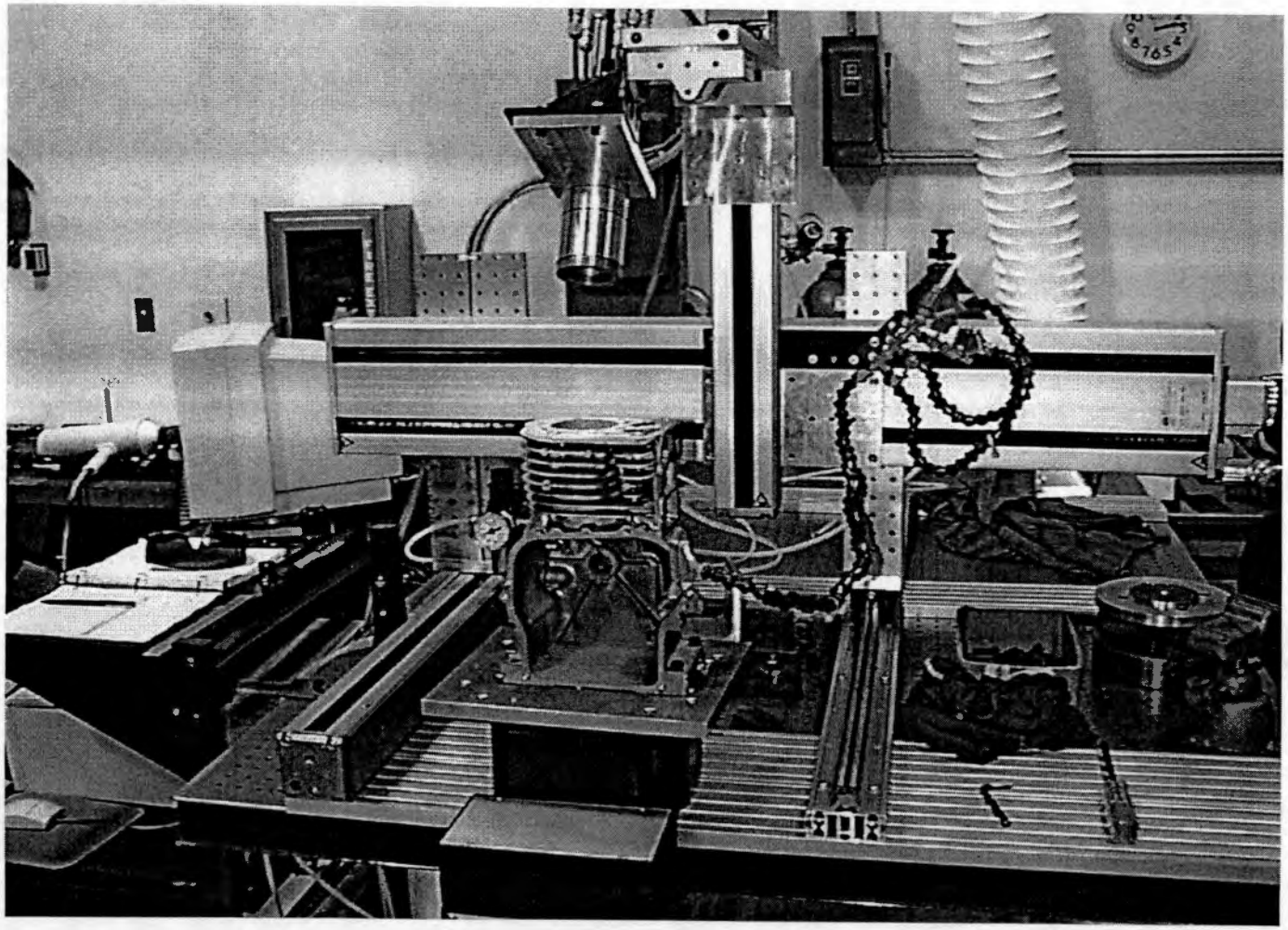


Figure 4: Laser Setup Before Processing.

4.2 Analysis Apparati

4.2.1 Lubricated Sliding Wear Tester

Lubricated sliding wear tests were performed using a custom-made wear tester [Figure 5]. The tests were of the block-on-wheel type. The wheel was 3.5 inches in diameter and made from A2 tool steel manufactured by Atlantic Stainless Company. It was then heat-treated to 63 R_c hardness. The surface of the wheel was smoothed to 800 grit roughness. The motor was a .75 horsepower electric motor manufactured by Leeson Electric Company. The lubricating oil was Halvoline SAE 10W-30, the same oil run in the test engine. Oil was applied to the wheel using a sponge submersed in oil. The wheel and sponge were kept in constant contact. This enabled a thin film of oil to be maintained on the wheel's surface. A four-pound normal load was applied to each sample. Each sample's wear surface was polished to 800 grit before testing. Tests were conducted at 1500 RPM and ran for eight hours.

Wear loss was determined by measuring weight loss of each of the samples. The samples were weighed before testing began, after four hours of testing and after a complete eight hours of testing. To insure oil had not been absorbed by the samples, after testing they were cleaned in an ultrasonic cleaner for thirty minutes. They were also thoroughly washed with both methanol and acetone following testing and before being weighed.

Overall weight loss was converted to volumetric weight loss to insure sample size was not a factor. This was calculated by dividing the overall weight loss by the density of aluminum, 2.7 g/cm^3.

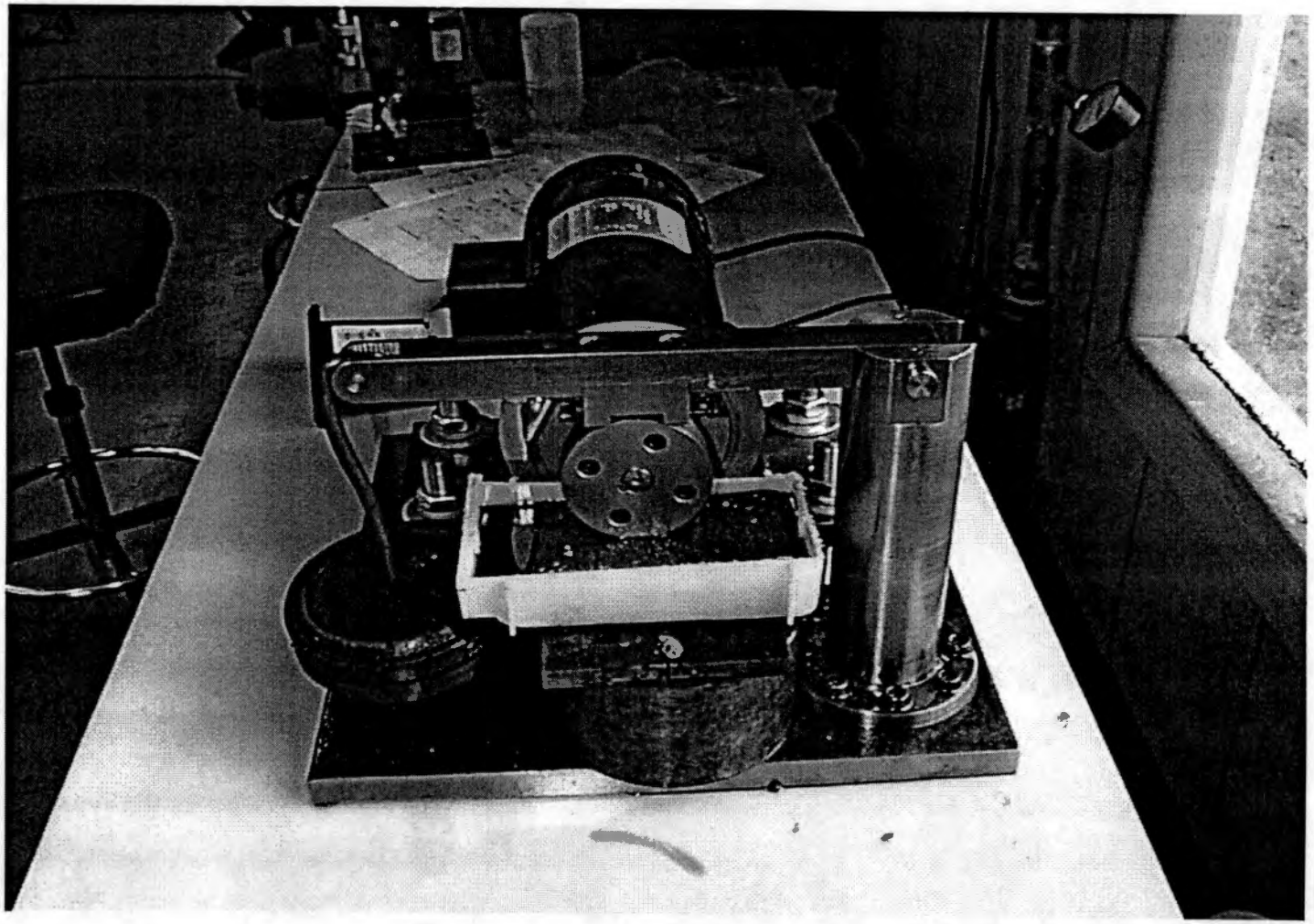


Figure 5: Lubricated Wear Tester.

4.2.2 Dry Sliding Wear Tester

Dry sliding wear tests were performed on each sample using a setup similar to the lubricated tests. The tests were also block-on-wheel type. The wheel was 3 inches in diameter and was constructed from A2 tool steel hardened to 60 R_c hardness. The motor was a .75 horsepower electric motor and manufactured by Dayton Electric Manufacturing Company. A four-pound load was applied to each sample. Tests were run at 1000 RPM. Each test lasted ten minutes, with the weight loss measured every two minutes. Weight loss for both dry and wet wear tests was measured using a digital scale manufactured by Sartorius Research Company accurate to the hundred-thousandth gram.

4.2.3 Microhardness Tester

A Buehler Micrometer was used for all microhardness tests. Available loads range from 10 g to 1 kg. All tests were performed at 500 g. The load was applied to the surface for 15 seconds for each mark that was made. Hardness marks were made in vertical columns every ten microns for the duration of the layer. Two columns were made per sample. The microhardness numbers were recorded in Knoops. All of the hardness values were averaged together to yield one hardness value for the sample.

4.2.4 Digital Imaging

A Nikon SMZ-U Zoom 1:10 microscope was used to magnify the image of the samples. Then an ELMO Color CCD TV camera was used to form the digital image.

This image was routed through a Panasonic S-VHS VCR to a computer, and images were then digitized using a Matrox Meteor frame grabber. An image tool designed by Matrox Electronic Systems Ltd. was then used to analyze the digital images.

4.2.5 Scanning Electron Microscope

The scanning electron microscope used for analysis of the samples was a Super-IIIA manufactured by International Scientific Instruments. Imaging and EDS analysis was performed using hardware made by IXRF systems. The software package Iridium v. 5.14, also manufactured by IXRF systems, was used for the analysis.

4.3 Engine Testing

The final stage of the experiment involved testing the final composition on an actual cylinder bore. For this the engine was placed on a dynamometer [Figure 6]. The dynamometer consisted of a water impeller connected to the output shaft of the engine. The flow of water could be adjusted to control the load placed on the engine. A throttle control was also present to adjust the speed of the engine. The engine was run at a constant load of 2.5 Horsepower at 3500 RPM. Exhaust temperatures and head temperatures were measured to insure the engine was running properly.

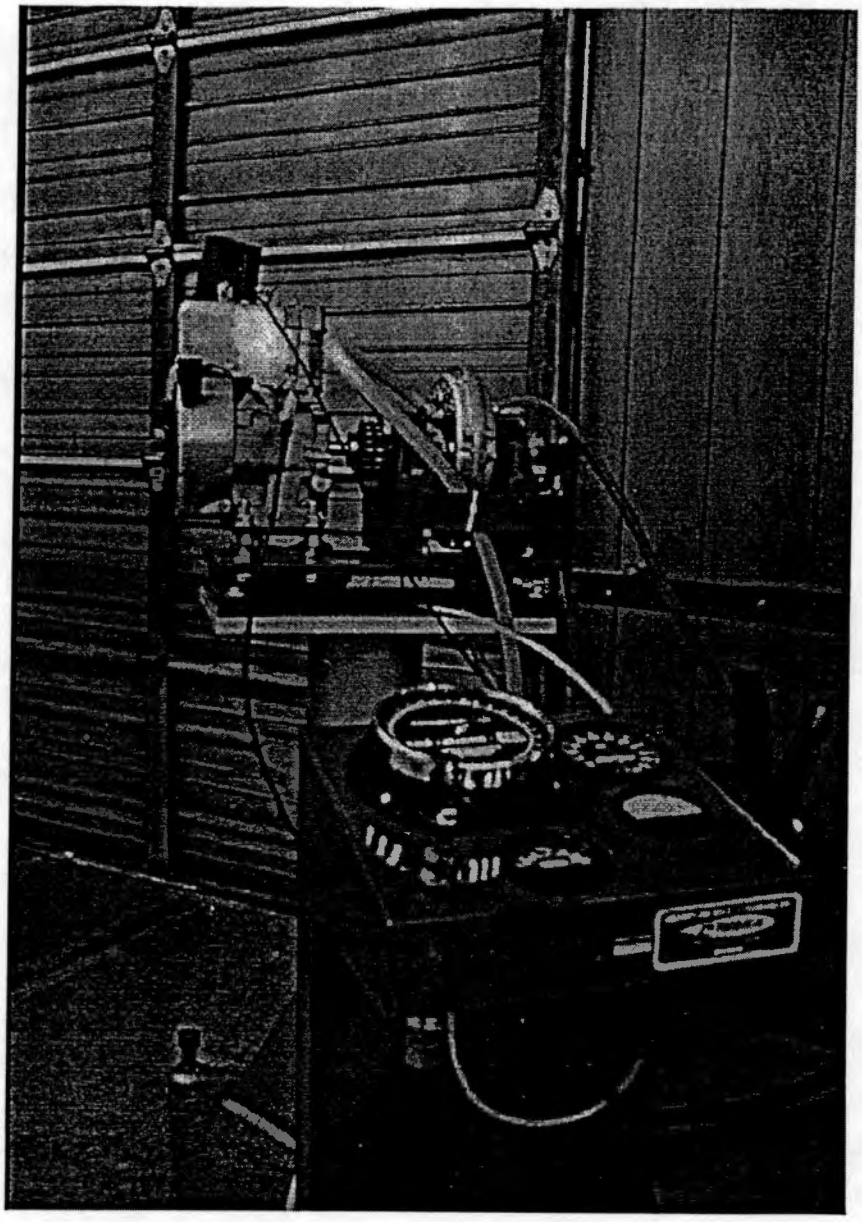


Figure 6: Engine on Dynamometer.

CHAPTER 5

RESULTS AND DISCUSSION

In Chapter 5 the results of the laser processing of both sets of runs are presented. These results include the layer depth, the composition, and the wear rates under both lubricated and unlubricated conditions.

5.1 Layer Depths

After the samples were processed, cross-sectional pictures were taken. These pictures often give an idea of the type of alloying that took place. It is sometimes apparent whether there was homogeneous or heterogeneous mixing. It can also be determined whether or not there was any porosity in the layer. From Figure 7 it can be seen that this aluminum contained some inherent porosity. However in this instance, they were mainly used as a device to analyze layer depths. Layer depths were measured at the deepest part of the layer [Figure 8]. The results from the cross-sectional photographs are displayed in Table 3.

It should be noted that the RDY 7443 group was sprayed with three coatings, yet still produced a thicker layer than the RDY 7444 group, which was sprayed with four coatings. This is due to human error. The samples were sprayed by hand and most likely the RDY 7443 group, while being sprayed one fewer time received more coating than the RDY 7444 group. The precursor thickness between coatings is relatively consistent. The RDY 7441 group was coated with a precursor thickness of

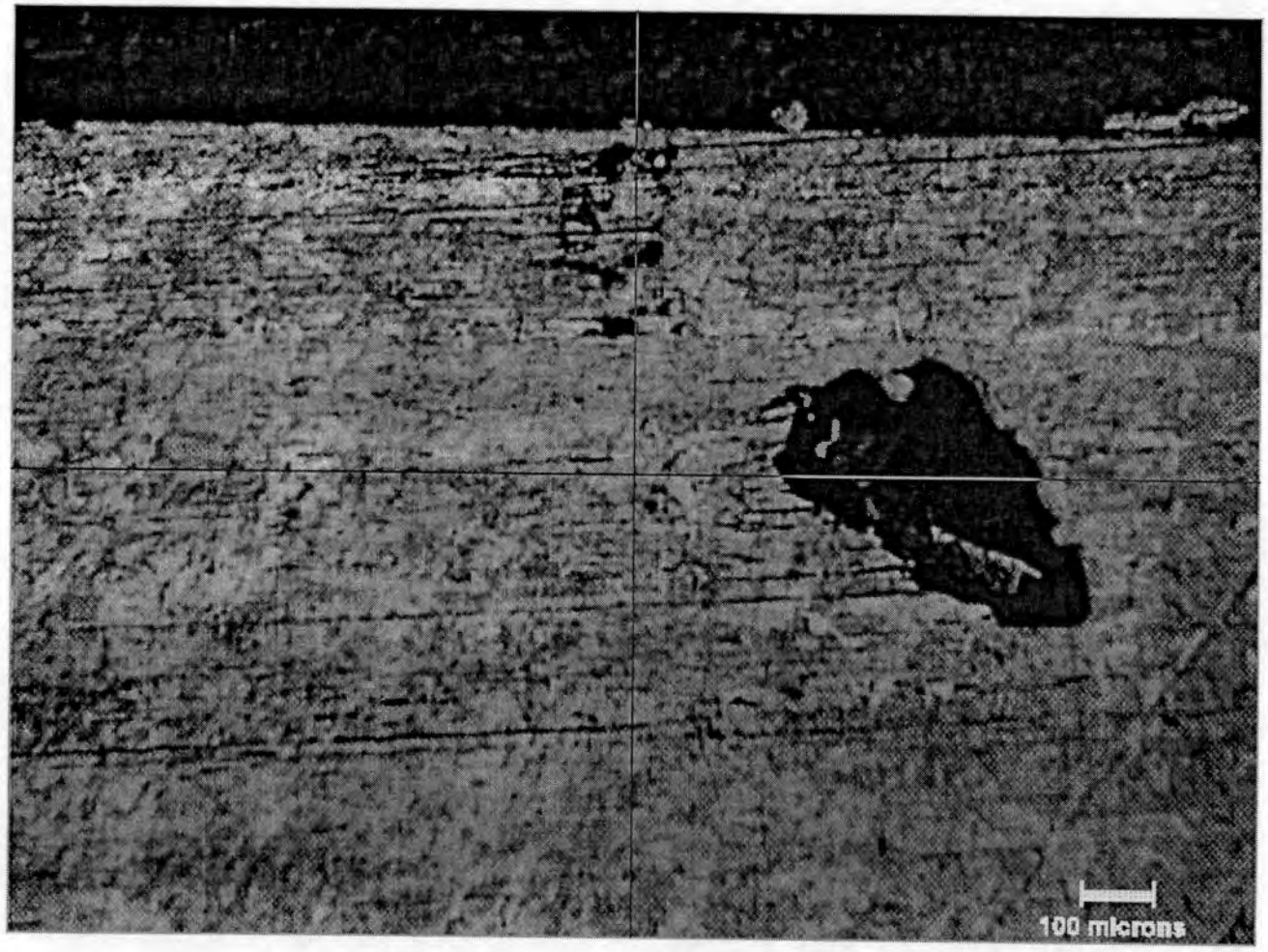


Figure 7: Cross Section of Unprocessed Aluminum 319 Showing Inherent Porosity.

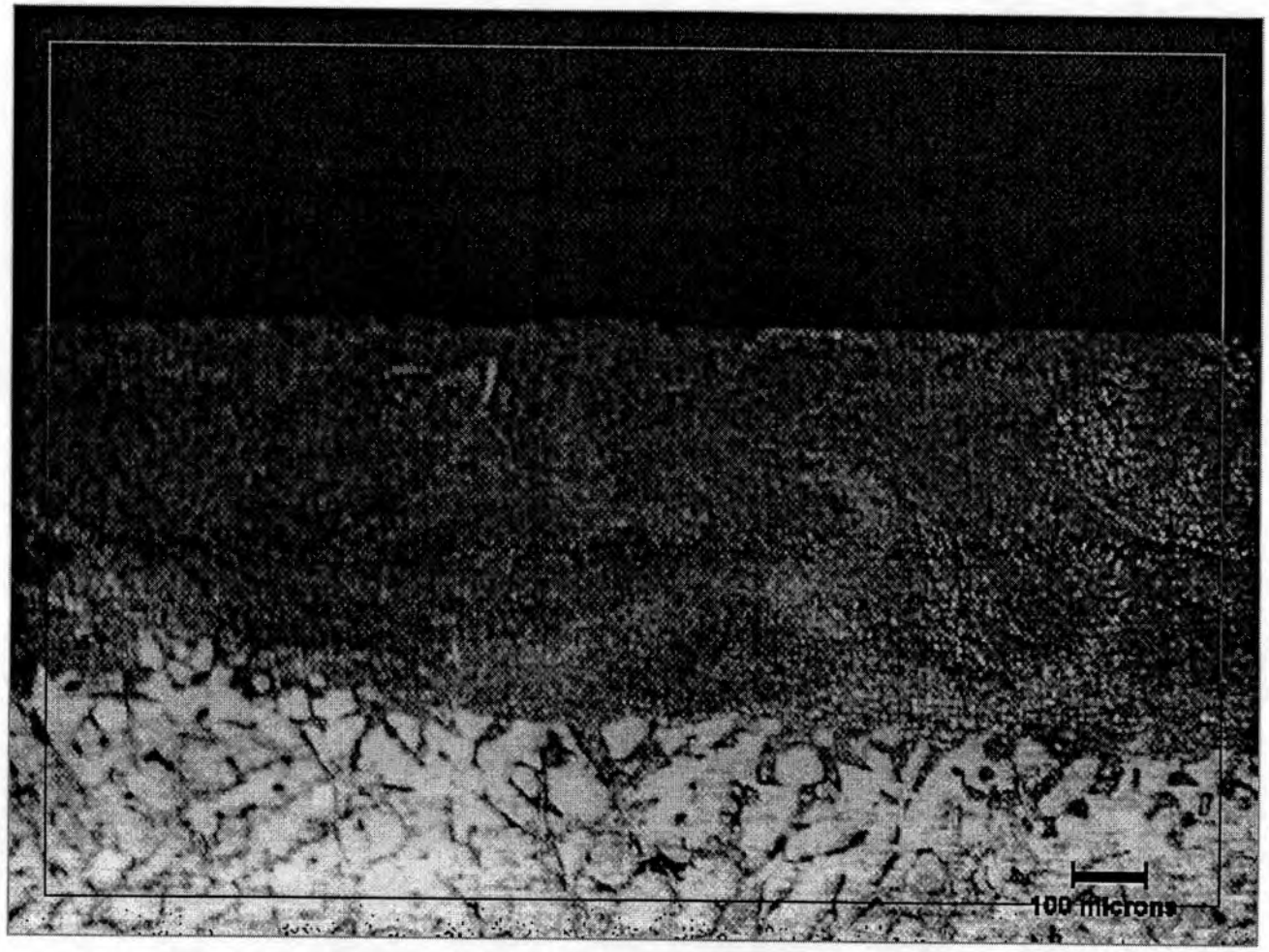


Figure 8: Cross Section of RDY 7445-2.

Table 3: RDY 744 layer depths, with conditions and rankings.

RDY #	Layer Depth (microns)	Power (Watts)	Speed (mm/min)	Precursor Thickness (microns)	Layer Depth Rank
7441-1	949	1750	3000	45	9
-2	853	1750	4500	45	17
-3	779	2000	4500	45	21
-4	1005	2000	3000	45	2
7442-1	965	2000	3000	66	5
-2	912	2000	4500	66	11
-3	875	1750	4500	66	15
-4	1105	1750	3000	66	1
7443-1	956	2000	3000	124	7
-2	758	2000	4500	124	23
-3	773	1750	4500	124	22
-4	949	1750	3000	124	8
7444-1	904	1750	3000	100	12
-2	934	1750	4500	100	10
-3	875	2000	4500	100	16
-4	883	2000	3000	100	13
7445-1	882	1750	3000	146	14
-2	699	1750	4500	146	24
-3	802	2000	4500	146	20
-4	964	2000	3000	146	6
7446-1	978	2000	3000	170	3
-2	824	2000	4500	170	18
-3	816	1750	4500	170	19
-4	971	1750	3000	170	4

45 μm. The next group had a thickness of 66 μm. The jump between RDY 7442 and RDY 7444 was the greatest at 34 microns. The difference between any two other consecutive groups was between 21 and 24 microns.

It is worth noting the average layer depths between samples processed at the same speed are remarkably similar. This can be seen in Table 4. The samples processed at 3000 mm/min and 1750 W have average layer depths within two microns of the samples processed at 3000 mm/min and 2000W. The same trend is apparent for samples processed at 4500 mm/min. This seems to indicate that in some instances layer depth is more a function of speed rather than power [Figure 9]. However, the layer depths of for all of the samples follow a linear trend when plotted against the power divided by the velocity (P/V) [Figure 10].

5.2 Silicon Content for RDY 744

The silicon content of each of the samples was measured using an EDS/SEM by taking point measurements at four separate locations within the layer. The compositional data received from these results show a few trends [Table 5]. Samples processed at the higher power and lower speed had the highest overall silicon content. The group with the lowest average silicon content was the group processed at the faster speed and lower power. This is because at lower speeds and higher powers, there is greater mixing of the precursor and the substrate. As the powers decrease and the speed increases, the less mixing occurs and hence less silicon in the final alloy.

However, the previous results were based on averages and there were certainly exceptions. For example, the group processed at 2000 W and 3000 mm/min

Table 4: RDY 836 processing conditions and layer depth.

Power (W)	Speed (mm/min)	Depth (microns)
1750	3000	956
2000	3000	958
1750	4500	825
2000	4500	825

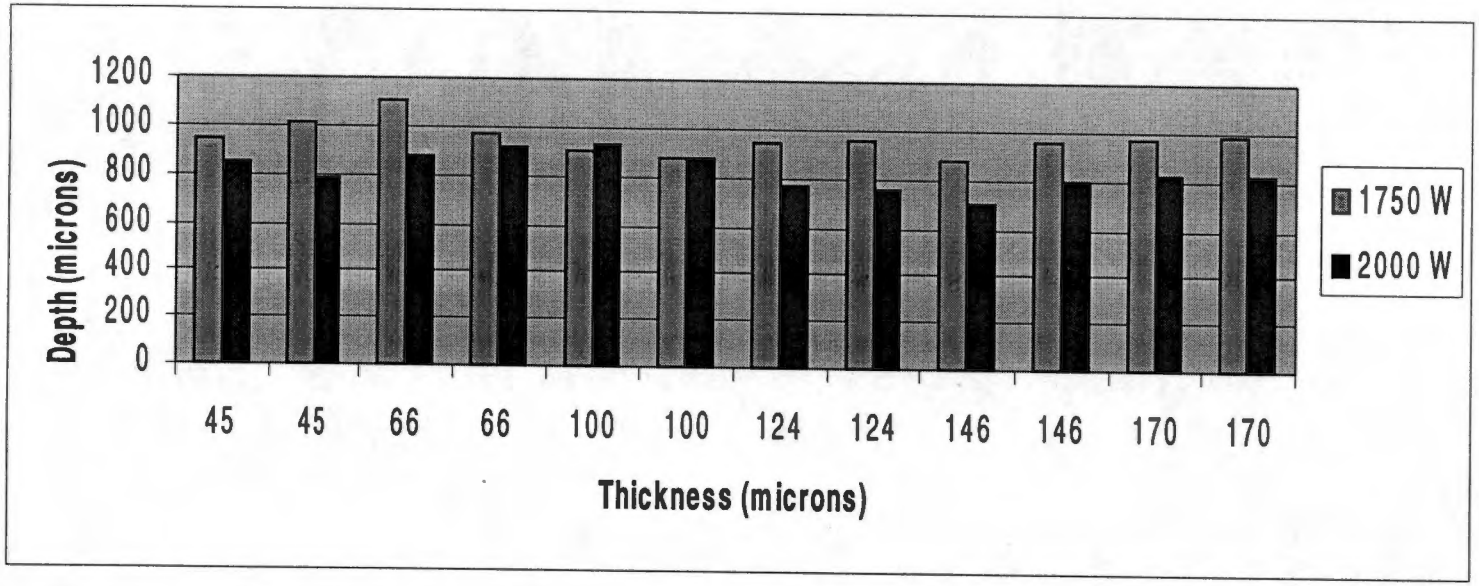


Figure 9: Layer Depth as a Function of Laser Beam Speed.

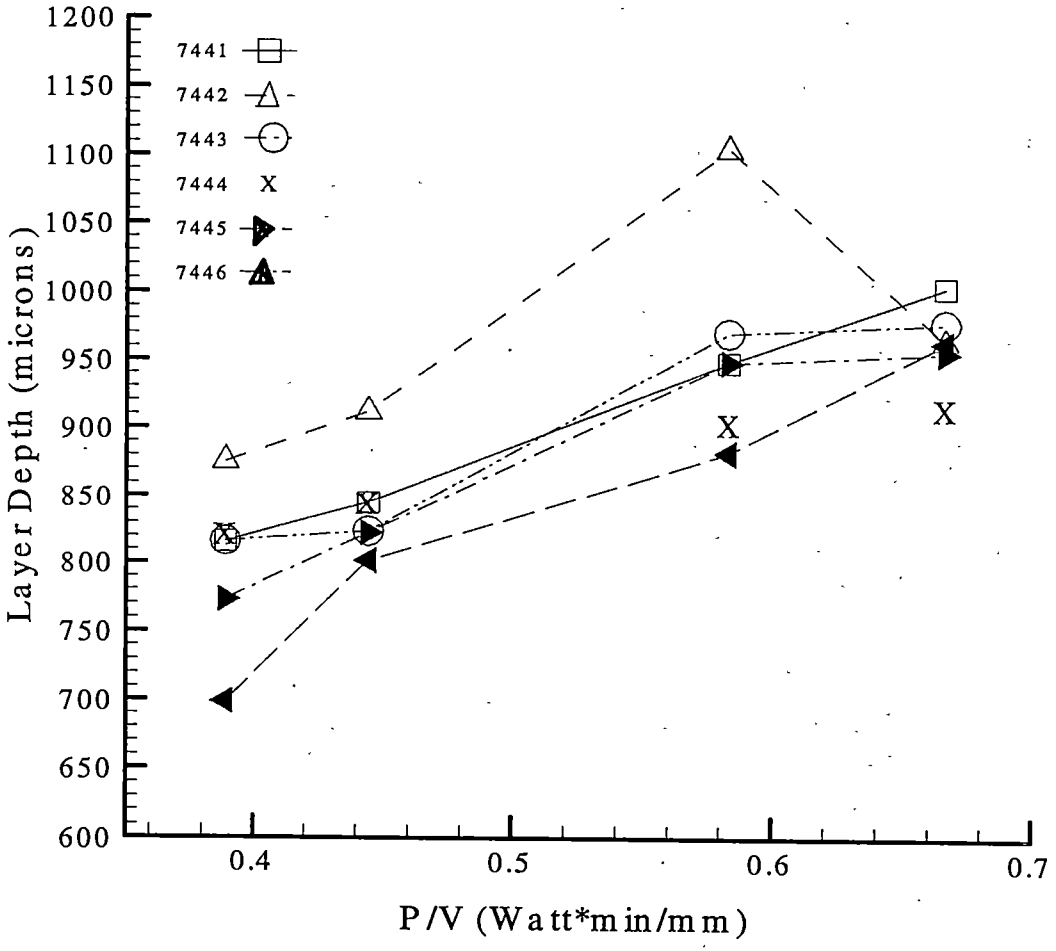


Figure 10: Layer Depth as a Function of P/V for RDY 744.

Table 5: Silicon content in RDY 744 samples.

	Si content Position 1 (wt. %)	Si content Position 2 (wt. %)	Average (wt. %)	Power (Watts)	Speed (mm/min)	Precursor Thickness (microns)	Layer Depth (microns)
7441-1	17	18	17	1750	3000	45	949
7441-2	14	18	16	1750	4500	45	853
7441-3	16	16	16	2000	4500	45	779
7441-4	9	8	9	2000	3000	45	1005
7442-1	16	15	15	2000	3000	66	965
7442-2	32	26	29	2000	4500	66	912
7442-3	19	19	19	1750	4500	66	875
7442-4	18	19	18	1750	3000	66	1105
7443-1	22	16	19	2000	3000	124	956
7443-2	21	19	20	2000	4500	124	758
7443-3	10	7	8	1750	4500	124	773
7443-4	24	22	23	1750	3000	124	949
7444-1	15	17	16	1750	3000	100	904
7444-2	15	13	14	1750	4500	100	934
7444-3	12	14	13	2000	4500	100	875
7444-4	33	41	37	2000	3000	100	883
7445-1	18	25	21	1750	3000	146	882
7445-2	21	28	24	1750	4500	146	699
7445-3	18	21	19	2000	4500	146	802
7445-4	24	19	21	2000	3000	146	964
7446-1	25	22	24	2000	3000	170	978
7446-2	17	23	20	2000	4500	170	824
7446-3	21	22	22	1750	4500	170	816
7446-4	21	18	19	1750	3000	170	971

had the highest average silicon content. The group which was processed at 1750 W and 4500 mm/min demonstrated the lowest average silicon content and included the sample with the smallest amount of silicon.

There also appears to be a small correlation between the silicon content and the precursor thickness. The RDY 7441 group, with the smallest precursor thickness showed the lowest median silicon content for any of the groups. RDY 7446 and RDY 7445 had the two largest precursor thicknesses respectively. They also had the two highest average silicon contents.

5.3 Silicon Content for RDY 836

The second set of samples were intended to duplicate RDY 7444-2, 7442-4, 7445-2, and 7444-4. They were run under the same processing parameters. Once processed, the precursor thickness was measured in several different places on each sample. It was found that in each case the precursor was within 26 microns of the desired thickness (120 and 146). This did not, however, guarantee that the silicon content would be similar. Tables 6 and 7 show the results of all eight samples processed in an attempt to duplicate the first four samples.

As can be seen from Tables 6 and 7, matching precursor thickness and processing parameters did not always yield similar average silicon content. However, two samples were processed for each sample intended to be duplicated and in every case at least one of these samples matched the intended silicon composition reasonably well. The layer depths of the RDY 836 group follow the same linear trend as the RDY 744 when plotted against P/V [Figure 11].

Tables 6 and 7: Silicon Content of RDY 836 and Layer Depth. Silicon Content Comparison of RDY 744 and RDY 836.

RDY	Power (W)	Speed (mm/min)	Precursor Thickness (microns)	Silicon Average (wt. %)	Layer Depth (microns)
836-1	1750	4500	65	15	647
836-2	1750	3000	65	20	765
836-3	1750	4500	120	24	757
836-4	1750	3000	120	29	831
836-5	2000	4500	110	32	691
836-6	2000	3000	110	32	831
836-7	2000	4500	95	23	699
836-8	2000	3000	95	23	816

RDY	Power (W)	Speed (mm/min)	Precursor Thickness (microns)	Silicon Average (wt. %)	RDY	Power (W)	Speed (mm/min)	Precursor Thickness (microns)	Silicon Average (wt. %)
836-1	1750	4500	70	15	7444-2	1750	4500	100	14
836-2	1750	3000	65	20	7442-4	1750	3000	66	18
836-3	1750	4500	120	24	7445-2	1750	4500	146	24
836-6	2000	4500	100	32	7444-4	2000	4500	100	38

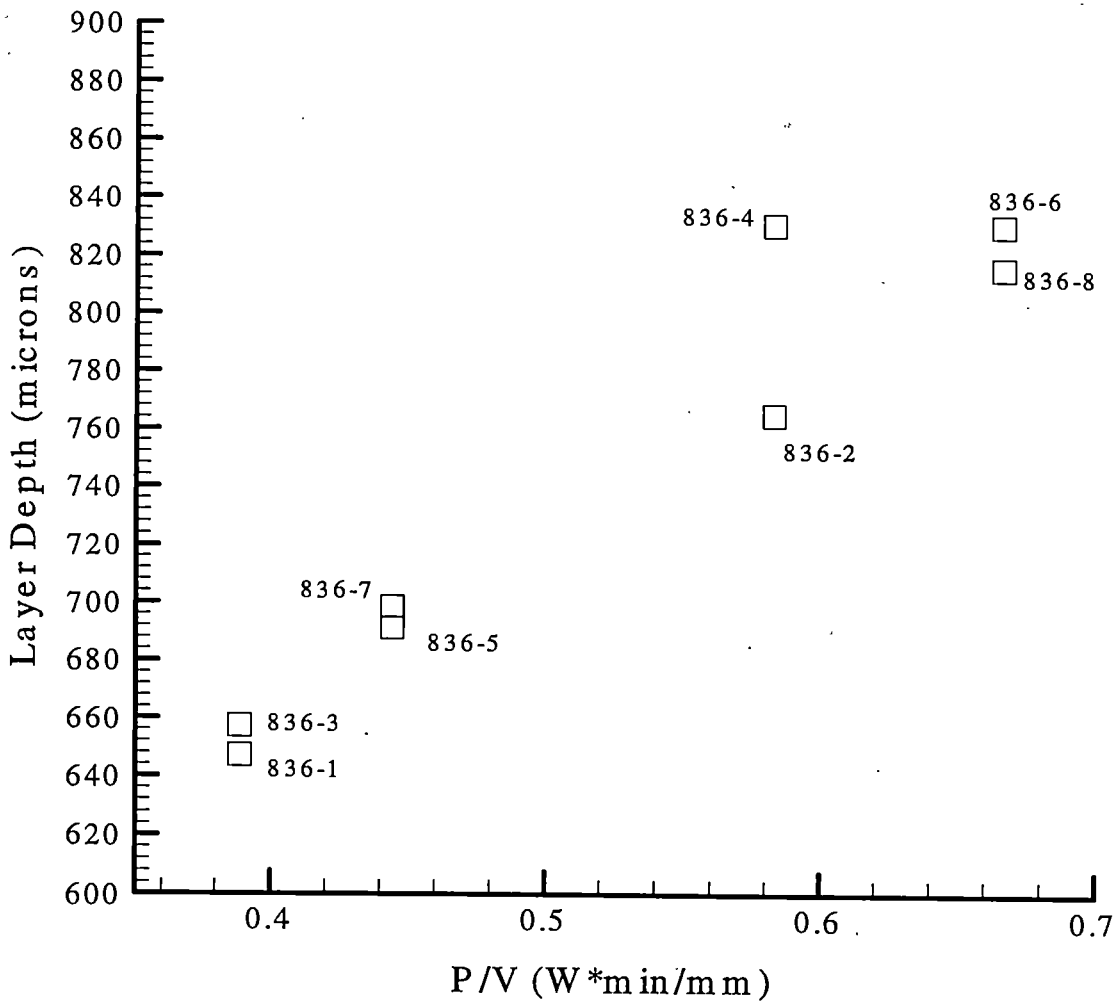


Figure 11: Layer Depth as a Function of P/V for RDY 836.

5.4 SEM Results for Eight Samples

A second set of EDS/SEM tests were taken after the matrix was reduced to eight samples. This second round of testing was intended to verify the results from the first set as well as offer more in-depth analysis of the remaining eight samples. First, compositional maps were taken of the entire layer to insure the silicon content measured at the four points was an accurate sampling of the entire layer. From Table 8, it can be seen that the results from the two methods were very similar.

The combination of compositional maps and point analysis taken for each of the samples show a higher silicon content at the top of the layer and then gradually decreasing. This can be seen in Table 9 and Figure 12. In Table 9, Point 1 was taken at a point near the top surface, Point 2 was taken in the middle of the layer, and Point 3 was taken near the bottom of the layer. Any point taken on a primary silicon particle was excluded. The primary silicon particles were measure to be approximately 5 microns in diameter. This is comparable to the more sophisticated production techniques for hypereutectic aluminum, but much smaller than what would be found in a typical casting.

In Table 9, the calculated silicon content was devised using the equation:

(27* Precursor Thickness + 6*(Layer Depth- Precursor Thickness))/Layer Depth

The 27 is the weight percent of silicon mixed in the precursor, while the 6 is the weight percent of silicon found in the A319 Al substrate. It should be noted that the calculated weight percent of silicon is, in most cases, far lower than what was measured using the SEM. This equation does not take into account the distribution of

Table 8: Comparison of Silicon Content Between Four Point Analysis and Compositional Map.

RDY #	Average of 4 Points (wt. % Si)	Compositional Map (wt. % Si)
7444-2	14	14
836-1	15	13
7442-4	18	17
836-2	20	19
7445-2	24	23
836-3	24	24
7444-4	37	35
836-6	32	31

Table 9: Silicon Content at Three Different Locations in the Layer.

RDY #	Point 1	Point 1 Depth	Point 2	Point 2 Depth	Point 3	Point 3 Depth	Calculated
	(wt. % Si)	(microns)	(wt. % Si)	(microns)	(wt. % Si)	(microns)	(wt. % Si)
7444-2	20	97	17	420	13	865	8.43
836-1	20	67	16	370	14	586	8.33
7442-4	22	77	19	405	14	1094	7.27
836-2	23	87	20	337	13	702	7.97
7445-2	35	93	24	353	20	662	10.63
836-3	33	90	22	321	18	717	9.51
7444-4	41	65	29	397	25	822	8.55
836-6	39	72	30	355	30	698	9.31

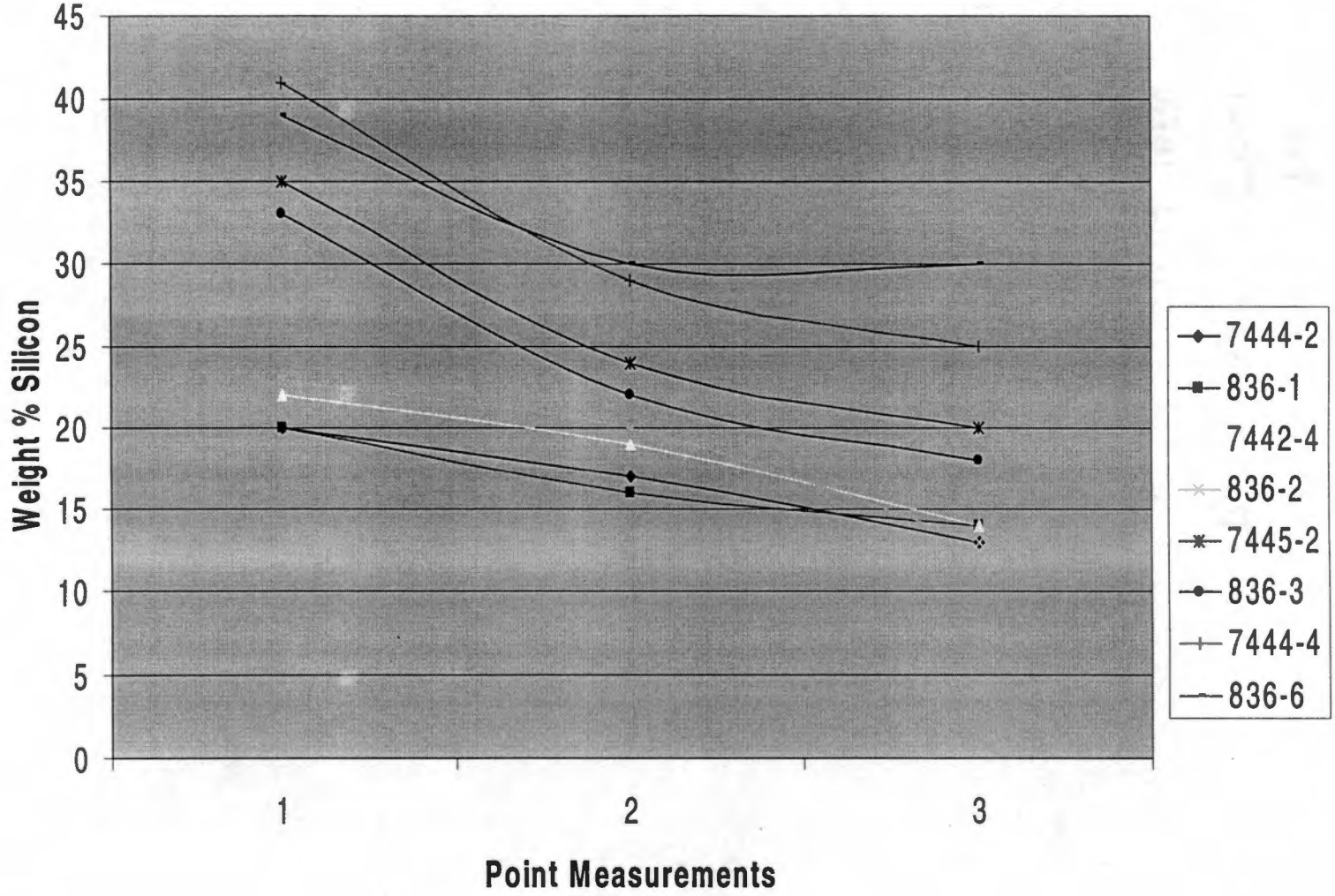


Figure 12: Silicon Content Distributed Through the Layer.

the silicon particles. As can be seen from Figure 13, the distribution of the silicon particles, throughout the layer is not uniform. The number of silicon particles and thus overall silicon content decreases significantly through the layer as can be seen from the point analyses in Figure 12 as well as the composition map, Figure 13. Using this equation, samples with larger layer depths will yield smaller silicon contents. While this may be true at the bottom of the layer, it is not representative of the entire layer.

The four samples with the highest near-surface silicon content were also the four samples with the highest values for power divided by laser translation velocity. RDY 7442-4 and RDY 836-2 had values for power divided by laser translation velocity (P/V) of .583 while RDY 7444-4 and RDY 836-6 had P/V values of .444. The remaining four samples had P/V values of .389.

5.5 Copper and Magnesium Compositions

As previously mentioned, the precursor contained copper along with the silicon. The copper compositions were measured at the same time as the silicon compositions, using the EDS/SEM. The copper compositions ranged from about 3 weight percent to about 8 weight percent. The magnesium compositions were between 1 and 2 weight percents. Neither appears to have had an effect on the wear performance of the samples. These results are found in Table 10.

Tables 10: Copper and Magnesium Composition.

RDY #	7444-2	836-1	7442-4	836-2	7445-2	836-3	7444-4	836-6
Cu %	3.7	3.83	3.5	5.42	5.12	5.17	6.01	7.58
Mg%	0.7	1.05	1.21	1.32	1.55	1.39	1.65	1.46

Table 11. Hardness Values of Laser Processed Samples.

RDY #	A1319	7444-2	836-1	7442-4	836-2	7445-2	836-3	7444-4	836-6
Hardness Hk(500)	95	116	118	119	136	138	134	141	151
Hardness rank	-	8	7	6	4	3	5	2	1
Si content	-	14	15	18	20	24	24	38	32
Si rank	-	8	7	6	5	3	4	1	2

5.6 Hardness Results

Once it was determined that there was a sample from the second group that matched up reasonably well with a sample from the first group, further testing was conducted. The first tests that were performed were hardness tests. The results are shown in Table 11.

These samples were ranked one through eight, with one being the hardest and eight being the least hard. These results are as expected with hardness being directly proportional to the silicon content [Figure 14]. The biggest discrepancy occurs between RDY 7442-4 and 836-2. There is only a one percent difference in silicon content, but there is a large difference in their hardness. Through SEM analysis it was shown that, although their silicon compositions are similar, there is more primary silicon present in RDY 836-2 than in 7442-4 [Figures 15 and 16].

5.7 Dry Wear Results

Dry wear tests were performed on these eight samples [Table 12]. From Figure 17, it can be seen that the wear of all but two of the samples is very close. The two samples containing the highest percentage of silicon performed far worse than any of the other samples did. While there was not a great deal of separation between the other samples, the sample with the least overall wear was 7445-2. Its final volumetric wear loss was almost an order of magnitude better than the base A319 Al. All samples outperformed unprocessed iron by at least a factor of two. Some samples with the least wear were up to three times better.

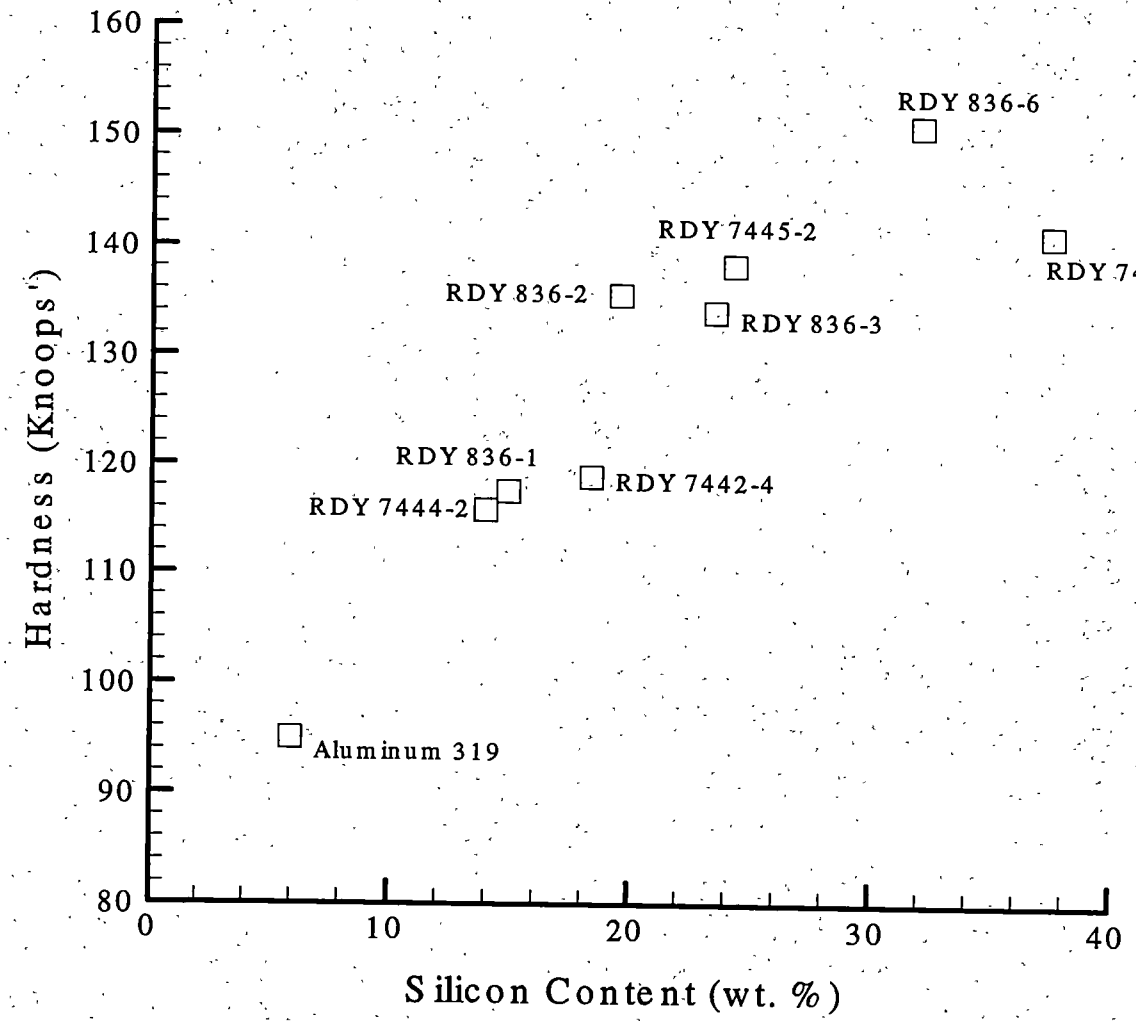


Figure 14: Hardness as a Function of Silicon Content.

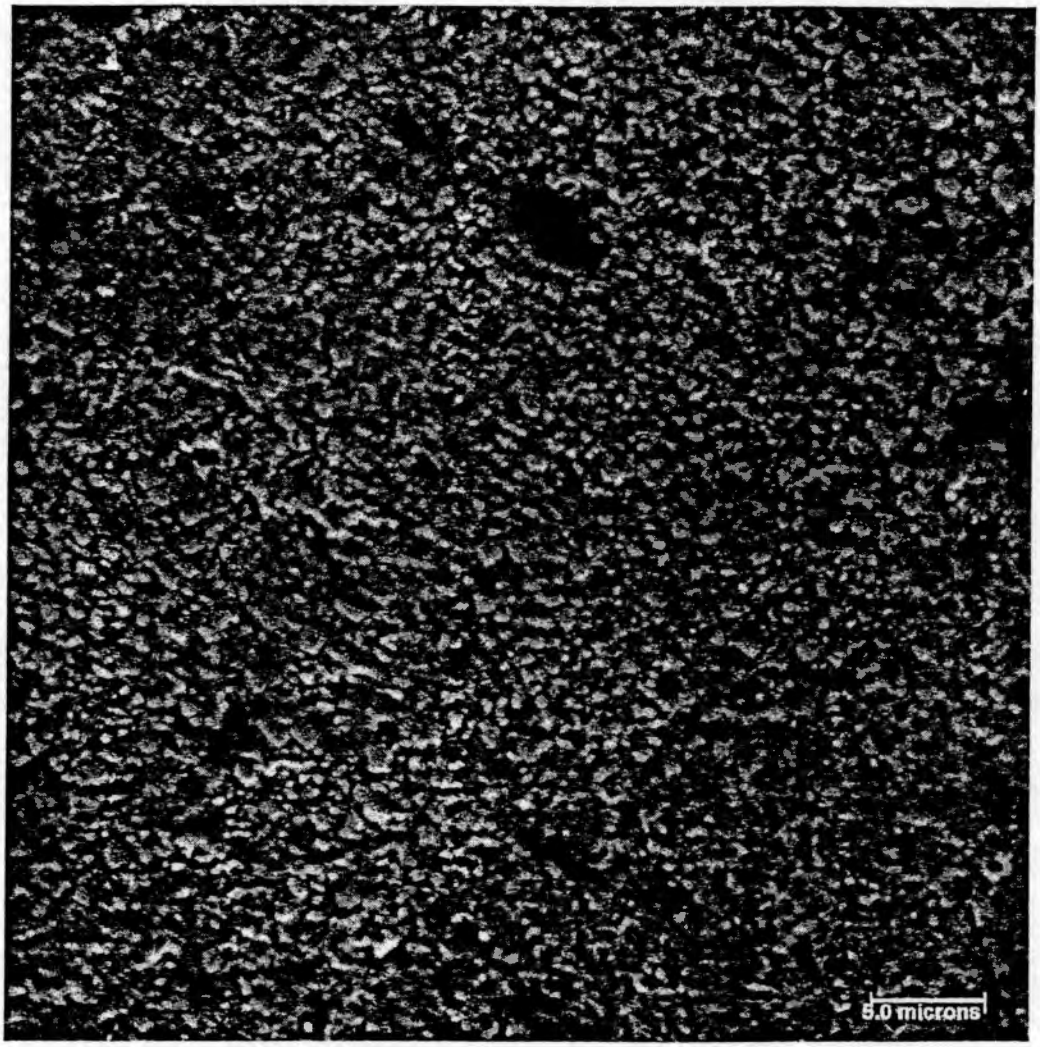


Figure 15: RDY 7445-2 at 2000 X.

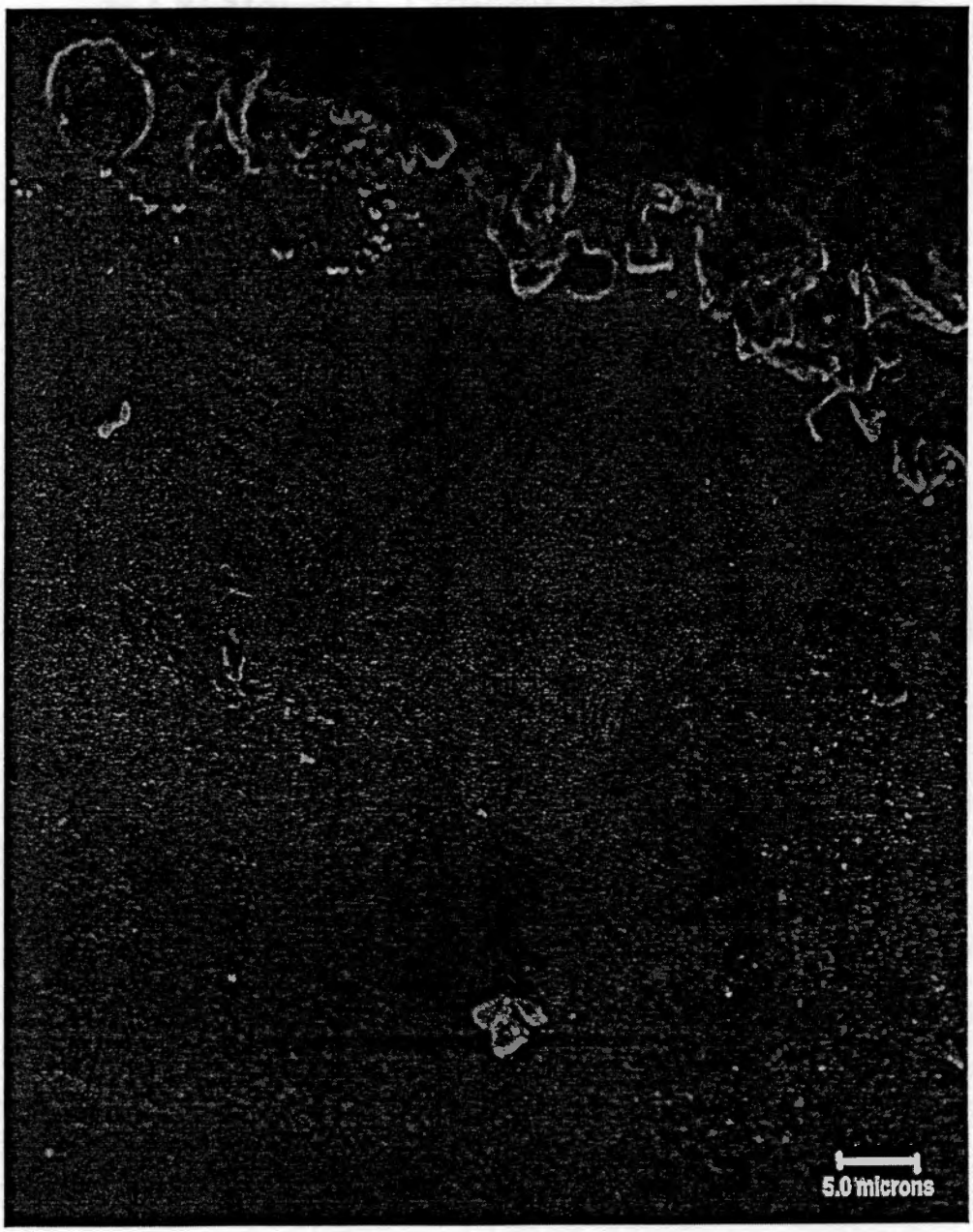


Figure 16: RDY 836-2 at 200 X.

Tables 12 and 13: Results from Dry Wear Tests. Temperature Measurements Recorded During Dry Wear Testing.

RDY #	Base 319	RDY 7444-2	RDY 836-1	RDY 7442-4	RDY 836-2	RDY 7445-2	RDY 836-3	RDY 7444-4	RDY 836-6
Volume lost (g/cm^3)	0.086022	0.008937	0.008926	0.009637	0.010048	0.008819	0.008907	0.011467	0.012904
Wear rank	-	4	3	5	6	1	2	7	8
Si content	-	14	15	18	20	24	24	38	32

Material Composition	Temperature (C)
A319 Al	229.0
14 wt. %	197.1
18 wt. %	196.5
24 wt. %	138.2
34 wt. %	173.2

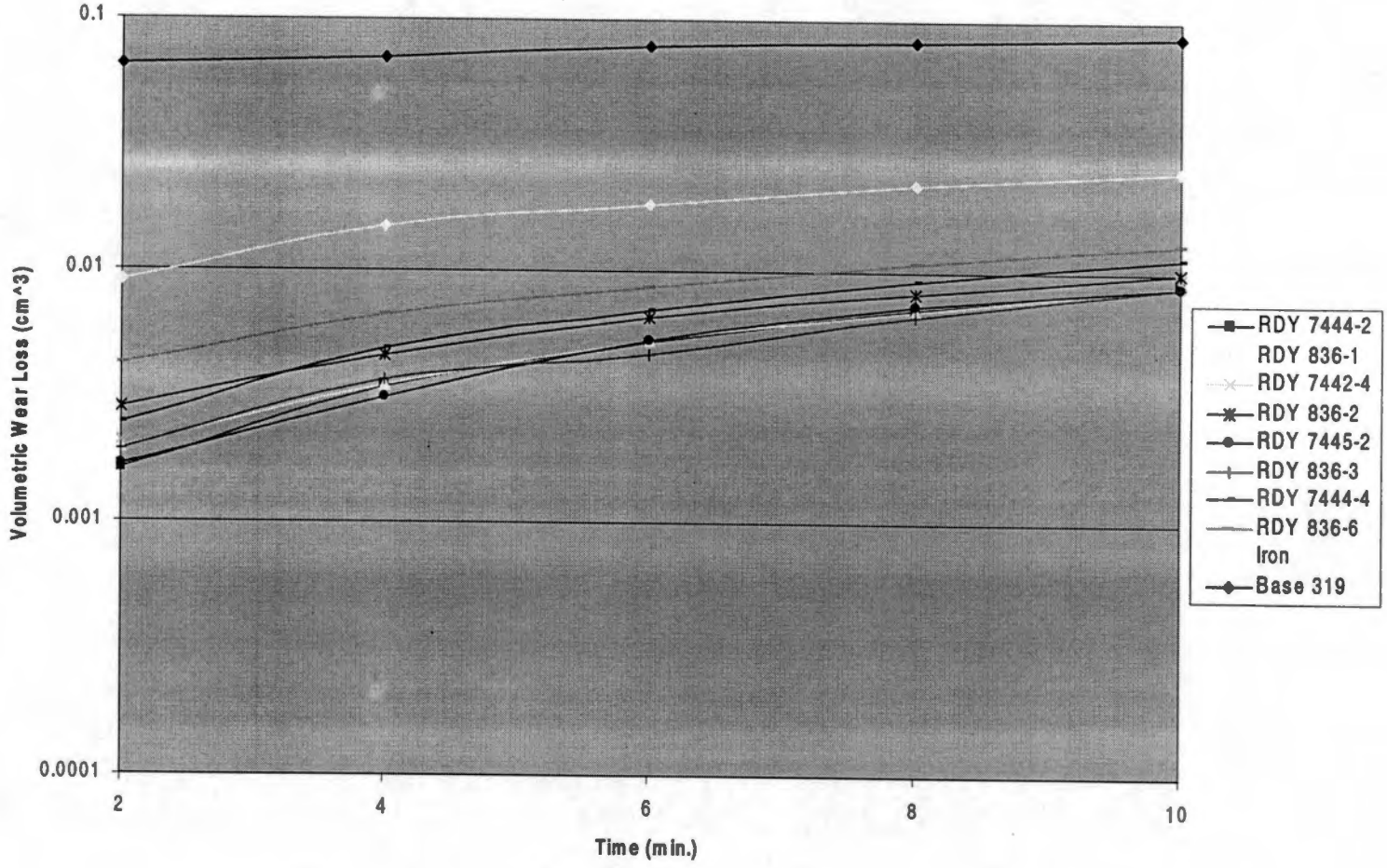


Figure 17: Volumetric Dry Wear Loss Comparison of Laser Processed Samples.

To help explain some of the differences during the dry wear tests, temperature measurements were taken after two minutes of testing. A thermocouple was adhered close to the friction surface using silver paint. The readout was displayed on a digital thermometer. The results are contained in Table 13 and plotted in Figure 18. The results are an average of the readings for both samples for each respective silicon weight percent. There was no more than five degrees deviation from the average for any of the samples.

Biswas and Reddy (1995) showed that the temperature at the surface of a material undergoing reciprocating sliding is related to the coefficient of friction. Their results indicate that the coefficient of friction is constant between 14-18 percent silicon, but drops off by 24 percent. In this study, the temperature at the surface of the samples was recorded. A similar trend is exhibited between the temperatures recorded in this study and the coefficients of friction recorded in Biswas and Reddy's (1995) study. In both studies, the 14 weight percent and 18 weight percent silicon samples exhibit similar qualities while the 24 weight percent sample is significantly lower. The temperature of the 24 weight percent silicon is about 70 percent of the 14 weight percent and 18 weight percent silicon samples. It is interesting to note that in this study the temperature rises for the 34 weight percent silicon samples.

Table 14 shows the silicon content of the samples taken by point measurement at near-surface locations and the volumetric wear rate of the samples after two minutes. The four samples, RDY 7442-4, 836-2, 7444-4 and 836-6, with the highest near-surface silicon content also had the highest volumetric wear rates for the first two minutes.

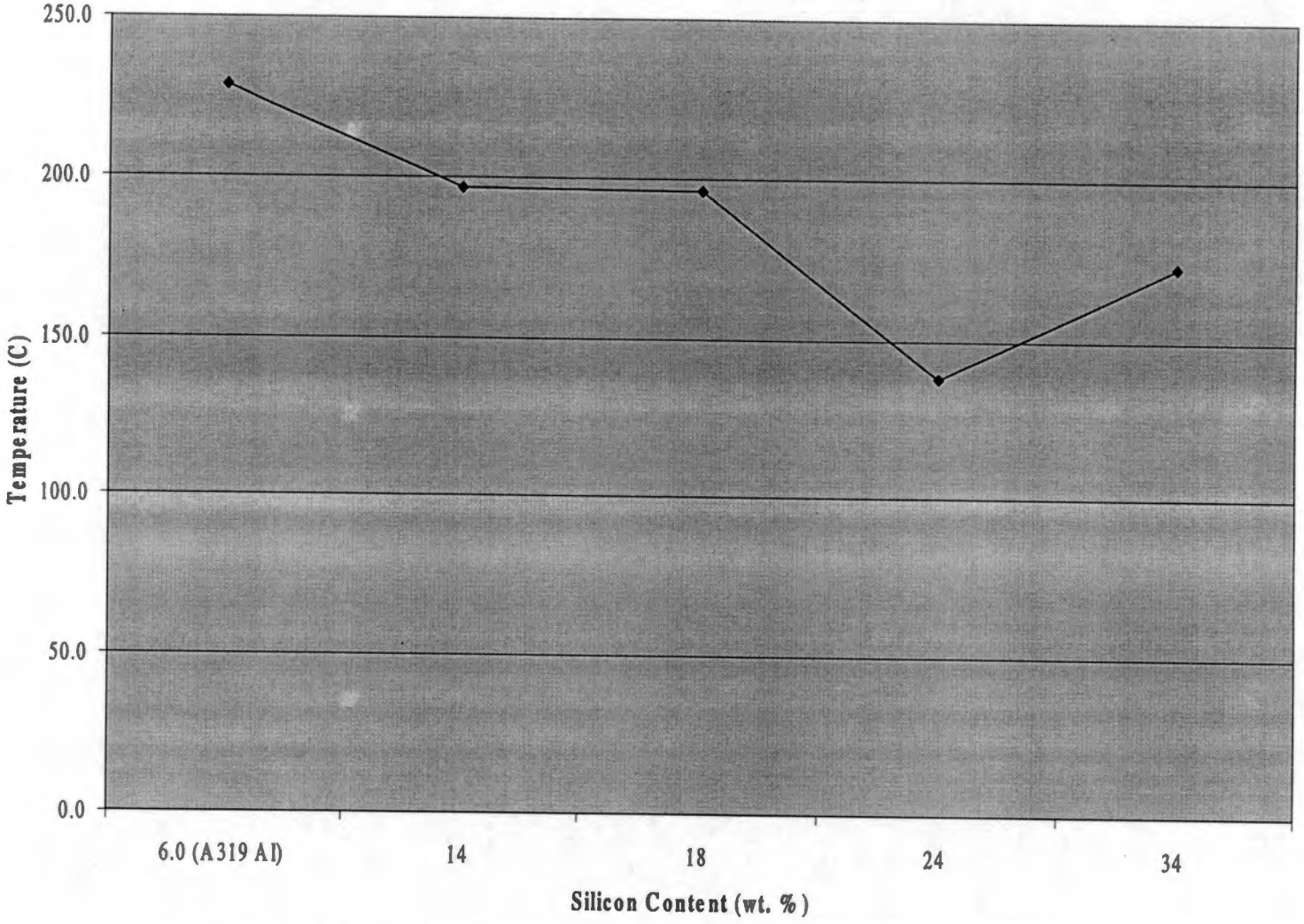


Figure 18: Dry Wear Temperature Measurements After Two Minutes of Testing.

Table 14: Silicon Content and Volumetric Wear Loss of Laser Processed Samples.

RDY #	Point 1 (wt. % Si)	Volumetric Wear Loss After 2 Minutes (g/cm^3)
7444-2	20	0.001641
836-1	20	0.001974
7442-4	28	0.002119
836-2	28	0.002889
7445-2	26	0.001704
836-3	25	0.001967
7444-4	41	0.002474
836-6	33	0.004315

5.8 Lubricated Wear Results

Lubricated wear tests were also performed on the eight processed samples as well as iron and unprocessed aluminum A319. The results from the lubricated tests closely resemble those from the dry wear tests. These can be found in Table 15 and Figure 19. Once again, the samples with the two highest silicon contents performed the worst. RDY 7444-4 and 836-6 had wear rates about 1.2 times higher than that of RDY 836-3. This was still far superior to unprocessed iron and aluminum. Each sample outperformed iron by at least 1.5 times and the wear rates compared to unprocessed aluminum were 1.8 times better.

5.9 Final Composition

It was decided that the composition that gave the best overall performance was the 24 weight percent. While there was not a large difference in wear rates between any of the processed samples, the 24 weight percent outperformed the others in both lubricated and dry wear tests as well as having a high hardness value. The 14 weight percent samples performed well on the wear tests, but had low hardness. The 18 weight percent samples performed well on the wear tests, but their hardness was inconsistent. The 34 weight percent silicon, while having high hardness values performed poorly on both sets of wear tests. The highest silicon content samples had high hardness, but poor wear. For these reasons, the 24 percent composition was chosen for the cylinder bore.

Table 15: Lubricated wear test results.

RDY #	Dry Wear (g/cm^3)	Rank	Wet Wear (g/cm^3)	Rank
Fe	0.025577		0.00091	
A319 Al	0.086022		0.00111	
RDY 7444-2	0.008937	4	0.00058	6
RDY 836-1	0.008926	3	0.000507	3
RDY 7442-4	0.009637	5	0.000544	5
RDY 836-2	0.010048	6	0.000526	4
RDY 7445-2	0.008819	1	0.000504	2
RDY 836-3	0.008907	2	0.000493	1
RDY 7444-4	0.011467	7	0.0006	7
RDY 836-6	0.012904	8	0.00061	8

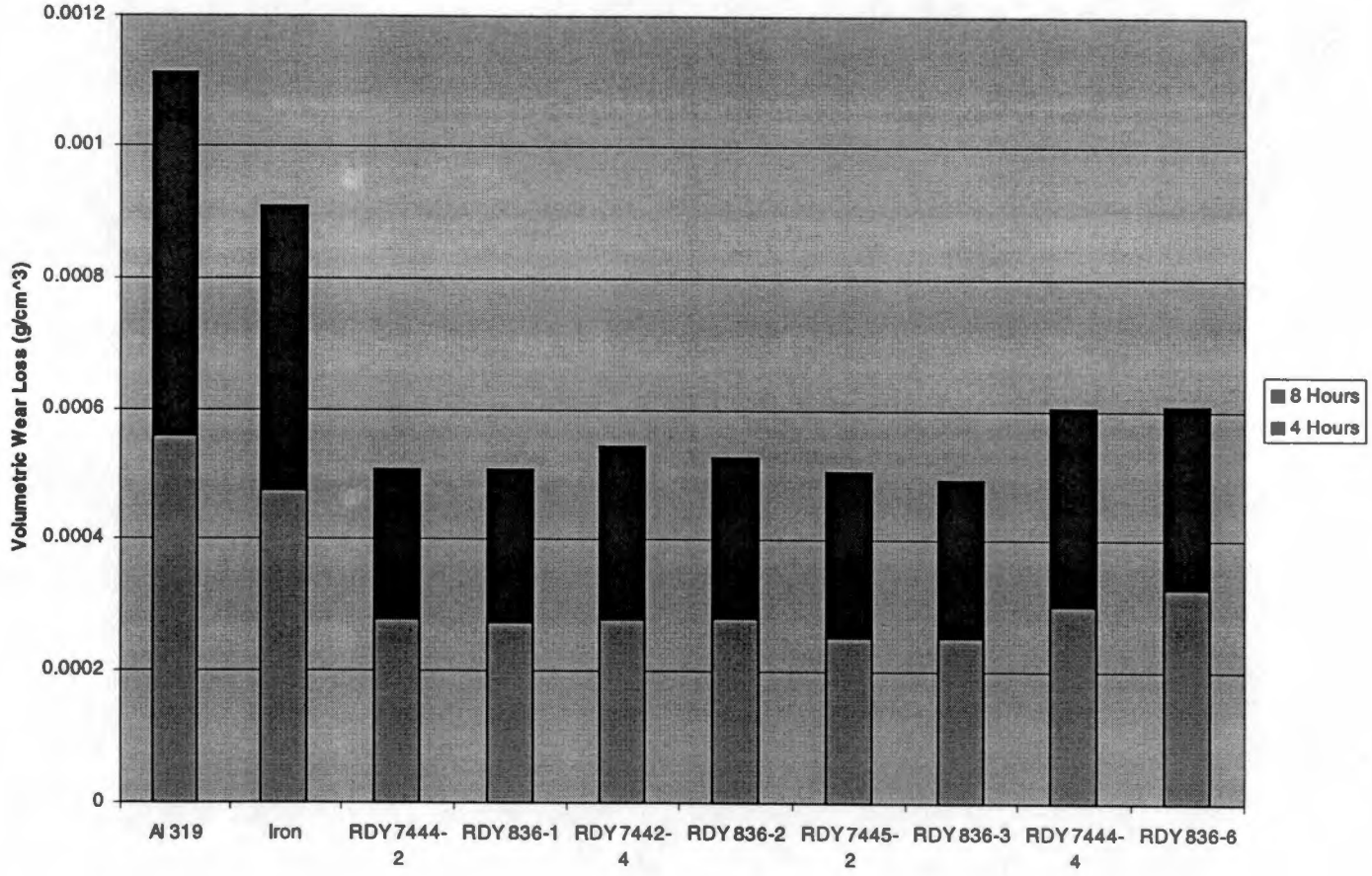


Figure 19: Lubricated Wear Comparison Between Iron, Aluminum and Laser Processed Samples.

5.10 Engine Bore Results

Two engine blocks were processed at the same conditions as the 24 weight percent silicon samples [Figure 20]. The first block to be processed contained a great deal of porosity that resulted in several groups of large holes [Figure 21]. These holes were so large, it was believed the surface of the cylinder wall had been compromised and the engine would not run properly. The second block, however, was of a different type of casting that contained less porosity on the cylinder wall. Most of this porosity was bunched together in two small groups [Figure 21]. The majority of the pores were small and were not thought to present a problem to the engine's performance.

The engine was tested for 60 hours on a dynamometer. The head was removed and cylinder bore dimensions were taken at 15 hours, 30 hours and 60 hours. Two measurements, 180 degrees from each other, were taken at the top, middle and bottom of the bore for a total of six different measurements. These results are plotted on Figure 22 and compared to results for an unprocessed cylinder run under the same conditions.

During testing, the compression within the cylinder bore increased dramatically. At the start of testing, the compression was 60 psi, by 50 hours it had increased to 90 psi. This seemed to correlate with an increase in engine oil consumption. For the duration of the test, engine oil consumption was higher than normal. This was thought to be due to the pores in the walls of the cylinder. The problem worsened to a rate of 16 ounces an hour as the testing duration reached 60 hours. For this reason, testing was stopped at 60 hours.

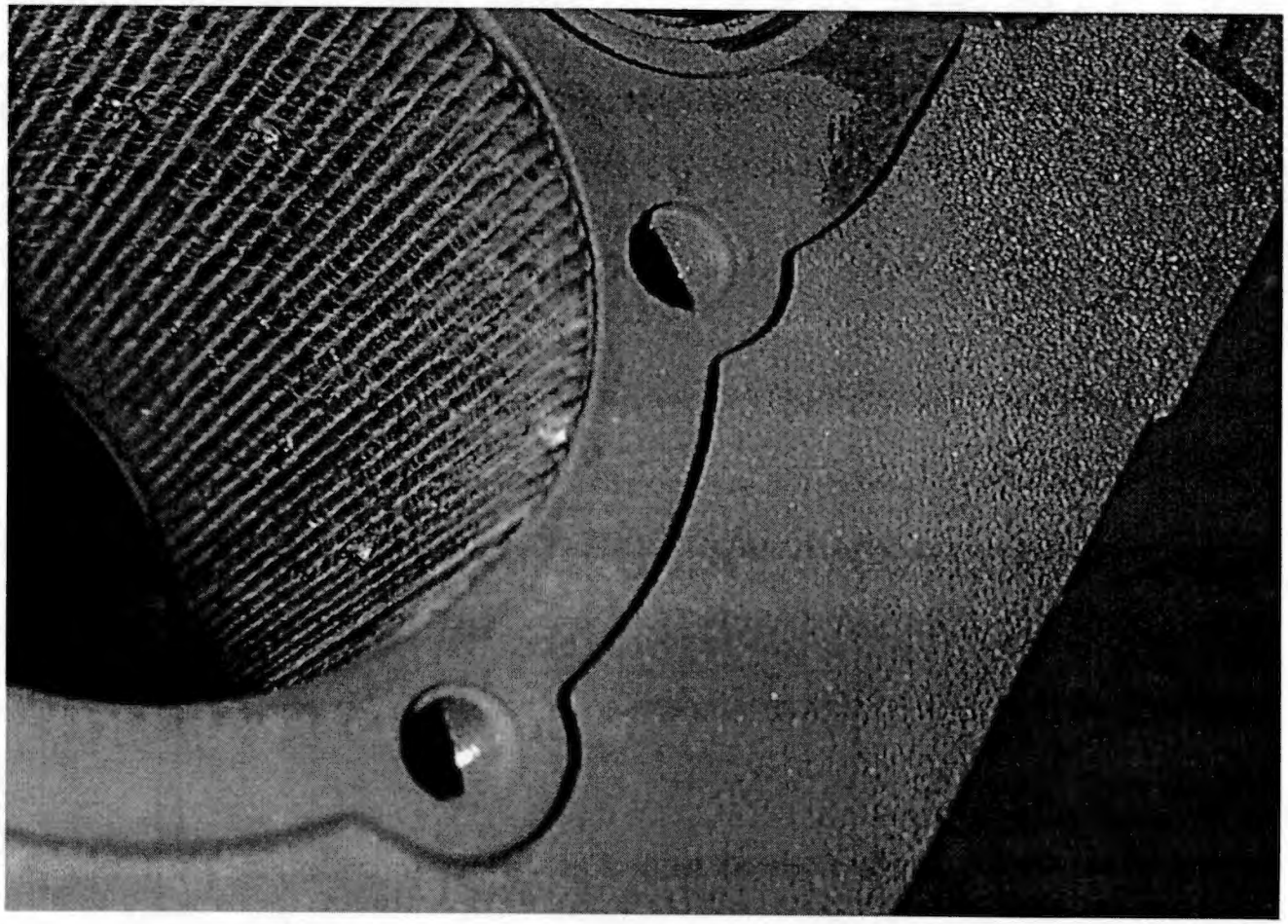


Figure 20: Closeup of Cylinder Wall of Block #1 After Processing.

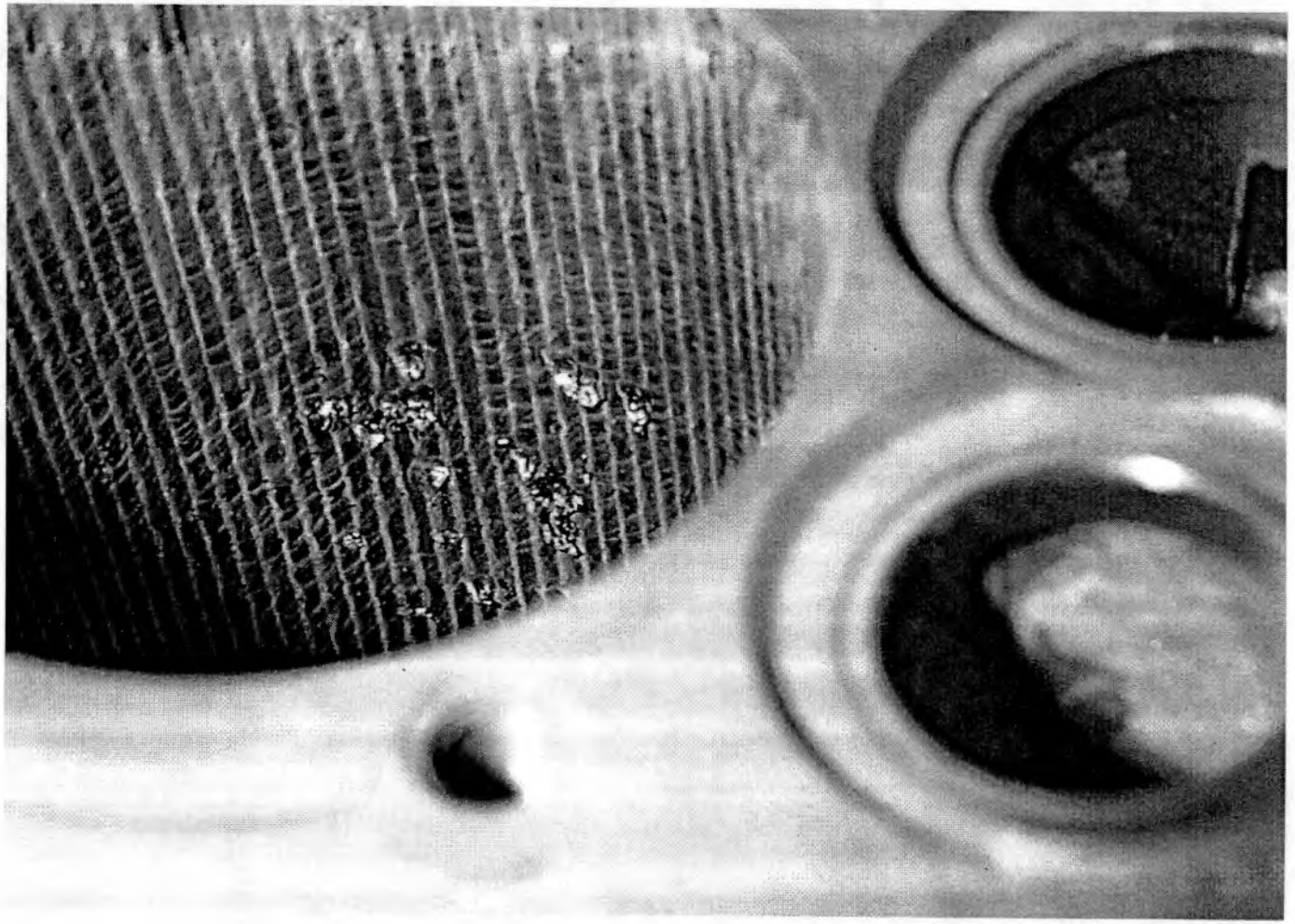


Figure 21: Closeup of Cylinder Wall of Block #2 After Processing.

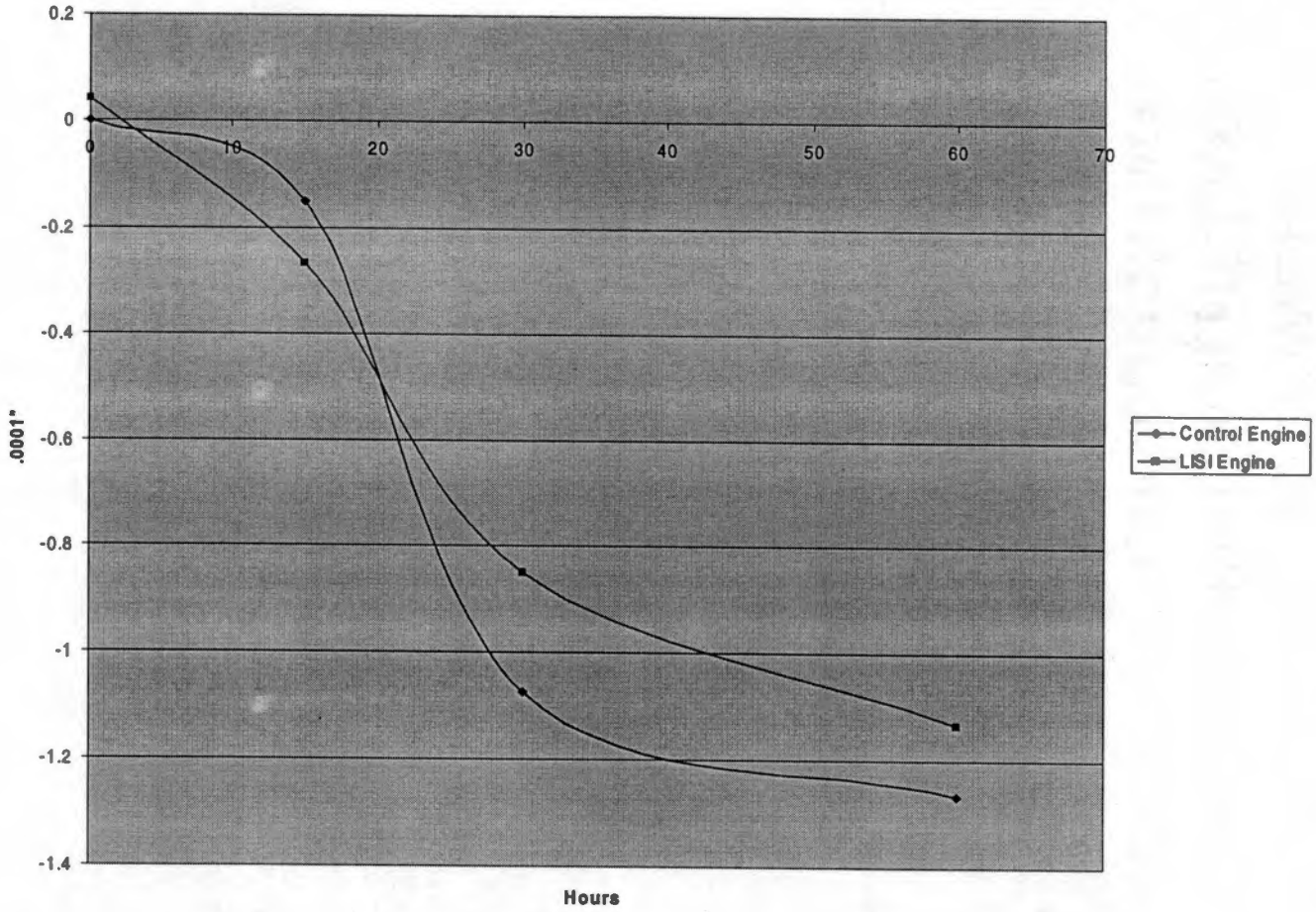


Figure 22: Wear Measurements of Control and LISI Engine.

5.11 Sources of Error

There are a several sources of discrepancy when laser alloying aluminum, including variations of the alloyed zone to due to inconsistencies in the metal. For example, a number of preliminary trials were discarded and the parameters repeated due to the amount of visible porosity. This porosity occurred in groups. That is, whenever it occurred there were many holes all within a relatively small area. This is most likely due to inherent porosity in the material, and was especially evident in the processing of the cylinder bores.

Error could also have been introduced by variations of the laser. A time period of seven months passed between the time the first data was collected and when the cylinder bore was processed. However, routine power measurements indicate there was low likelihood of significant differences between processing trials.

There also could have been error introduced in the measuring of the thickness of the precursor on the samples. The precursor was measured in two different places on each sample after processing. For the most part, these measurements were very consistent between the two different measured areas. However, the precursor could have been slightly thinner or thicker at other places on the sample.

CHAPTER 6

CONCLUSIONS

The results of the study, sources of error in the study, and options for future work are discussed in this chapter.

6.1 Results

It was determined through this experiment that the hardness and the sliding wear rate of aluminum A319 is improved through the addition of silicon and other materials through the LISI process. Hardness, in the processed region, is dependent upon the sample's silicon content, and layer depths are a function of the laser power divided by the laser translation velocity.

The dry sliding wear performance of the aluminum samples was improved by almost an order of magnitude over the unprocessed aluminum A319 and by a factor of three over iron. During lubricated sliding wear, the LISI samples demonstrated wear performance twice that of unprocessed aluminum and 1.8 times better than iron.

SEM analysis of the samples showed that there was decreasing silicon distribution from the top to the bottom of the layer. The increased silicon content at the surface improved wear performance. It was also shown that the silicon particle size (approximately 5 microns) was similar for all of the samples regardless of overall silicon content. This is consistent with other research that has focused on production of small particle sizes for improved wear resistance. From this it is determined that

LISI is a viable technique for producing a fine matrix of silicon particles, thus improving wear performance.

While some samples did perform better than others during wear tests, there was not much discrepancy between the 14-24 weight percent silicon samples. In accordance with Biswas (1995), it can be concluded that sliding wear is consistent over the range of 14-24 weight percent silicon. This is true for both dry and lubricated tests. However, somewhere between 24 and 31 weight percent silicon, wear is adversely affected. This was thought to be due to the excessive amounts of silicon in the upper portion of the processed region. As sliding contact is made between the sample and the wear surface, the silicon is pulled out of the alloyed material resulting in large portions of material removal unlike the cases with lower silicon contents.

The pores in the cylinder bore surface were caused by inherent porosity in the base material. Since the cylinder bore was pitted, the rings were never able to seat correctly resulting in higher than normal oil consumption. The results that were obtained from the engine testing show that laser processing the cylinder bore does improve wear. However, the duration of the testing was not long enough to demonstrate how much improvement would take place over extended periods of time.

6.2 Future Work

There is still a great deal of work to be done in the area of improving wear in the cylinder bore using laser processing. Most of the research would be centered on production. There are many issues, most of which were not addressed in this paper, which would need to be dealt with in order to make this process production ready.

One issue would be spraying. Currently, all spraying is done by manually. There is a limit to the degrees of consistency that can be maintained this way. Other options, such as automated spraying, need to be considered.

Another issue that needs to be considered involves porosity. It is difficult to determine how a specific sample is going to behave during processing. There are times when, after processing, there is so much porosity that the samples would not be adequate for use in a cylinder. This raises the questions of how much porosity is too much for use in an engine and how a poor casting could be identified before processing.

One area in need of further examination is to define the point at which wear is adversely affected by silicon content. This paper, as well as other work, has shown that wear rates up to 24 weight percent are consistent, but somewhere between 24 and 31 weight percent silicon, the wear performance is hindered. A determination of the cause of and exact placement of this transitional point would be beneficial.

BIBLIOGRAPHY

BIBLIOGRAPHY

1. Advanced Materials, Volume 19, October 13, 1997.

2. American Society for Metals, Metals Handbook Ninth Edition, Volume 2 Properties and Selection: Nonferrous Alloys and Pure Metals, 1979.

3. Alpas, A.T., Metallography of Sliding Wear in SiC Reinforced Aluminum Matrix Composites, Microstructural Science, Volume 19, 1992.

4. Ames, W., Alpas, A.T., Wear mechanisms in hybrid composites of graphite-20% SiC in A356 aluminum alloy (Al-7% Si-0.3% Mg), Metallurgical and Materials Transactions, January 1995.

5. Andrews, J.B., Seneviratne, M.V., Jett, T.R., The Influence of Silicon Content on the Wear Characteristics of Hypereutectic Al--Si Alloys, Wear of Materials, 1985.

6. Blank, E., Hunziker, O., Mariaux, S., Load Bearing Capability of Laser Surface Coatings for Aluminium--Silicon Alloys, Laser Treatment of Materials. ECLAT '92, DGM Informationsgesellschaft mbH, 1992.

7. Blank, E., Pierantoni, M., Carrard, M., Laser Surface Modification of Al--Si Cast Alloys for Wear Resistance and Surface Toughness, Surface Modification Technologies III, 1990.

8. Biswas, S.K., Reddy A.S., Wear and seizure of aluminum-silicon-based IC engine component materials, Journal of the Indian Institute of Science, January-February 1996.

9. Bretta,T., www.bestweb.net/~bretta/v8shortblock.htm

10. Coquerelle, G., Friction and Wear of Laser Treated Aluminum-Silicon Alloys, European Conference on Laser Treatment of Materials, 1986.

11. Davis, F.A., Eyre T.S., The Effect of Silicon Content and Morphology on the Wear of Aluminum-Silicon Alloys Under Dry and Lubricated Sliding Conditions,Tribology International, 1994.

12. Donahue, R. J., Cleary, T. M., Shaeffer, B. L., Internal combustion engine having a hypereutectic Aluminum-Silicon block and Aluminum-Copper pistons', U.S. Patent No. 5,253,625, October 1993.

13. Eyre, T.S., Dutta, K.K., Davis, F.A., Characterization and Simulation of Wear Occurring in the Cylinder Bore of the Internal Combustion Engine, Tribology International, 1990.

14. Genualdi, A., Aluminum Casting Metallurgy, Saturn Course #5767, 1997.

15. Ghosh, Kunal, McCay, M.H., Dahotre, N.B. "Formation of a Wear Resistant Surface on Al by Laser Aided In-situ Synthesis of $MoSi_2$." Journal of Materials Processing Technology, Accepted for Publication November, 1998.

16. Hill, S. H., Hartfield-Wunsch Susan E., Tung, Simon C., Bench Wear Testing of Common Gasoline Cylinder Bore Surface/Piston Ring Combinations, Tribology Transactions, Volume 39, 1996.

17. Hofmann, H.H., Aluminum Engine Blocks: Some Design Considerations, Automotive Engineering, February, 1983.

18. Hopkins, J.A., McCay, M.H., Dahotre, N., Performance of Laser Processed Aluminum Alloys for Engine Bore Applications, SAE #980458, 1998.

19. Hopkins, J.A., Murray, M., McCay, M.H., Laser Processed Aluminum Surfaces in Automotive Applications: Performance Requirements for Cylinder Bores and Valve Seats, SAE #980435, 1998.

20. Jorstad, J.L., Hypereutectic Al-Si Casting Alloys: 25 Years, What's Next?, Metals Abstracts, April, 1996.

21. Kennedy, N., Duncan, D., Evaluation and classification of performance of laser surface processed aluminum A319 samples, 1997.

22. Massinon, D., Constantin V., Adam, R., Tribological Characteristics and Wear Mechanisms of Hypereutectic Alloys, SAE #970189, 1997.

23. Megaw, J.H.P.C., A.S. Bransden, Trafford, D.N.H., Surface Cladding by MultiKilowatt Laser, International Colloqium on Welding and Melting by Electrons and Laser Beams, 1983.

24. Okabayashi, K., Kawamoto, M., Influences of Silicon Content and Grain Size of Primary Silicon Crystals on the Wear of High Silicon Aluminum Alloys, Bulletin of University of Osaka Prefecture, 1968.

25. Okabayashi, K., Kawamoto, M., Notani, H., Study on Wear of Casting Aluminum Alloys, Bulletin of University of Osaka Prefecture, 1966.

26. Reddy, A.S., Pramila Bai, B.N. & Murthy K.S.S., Wear and Seizure of binary Al-Si alloys, Wear, January 1994.

27. Sarkar, A.D., Wear of Aluminum-Silicon Alloys, Wear, Volume 31, 1975.

28. Stone, Richard, Introduction to Internal Combustion Engines, Second Edition, Society of Automotive Engineers, 1992.

29. Scarlett, M., Jaguar V-8, Automotive Engineer, June-July 1996.

30. Tomlinson, W.J., Bransden, A.S., sliding Wear of laser alloyed coatings on Al-Si 12%, Journal of Materials Science Letters, Volume 13, 1994

31. Tomlinson, W.J., McAra, J.R., Bransden, A.S., Fabrication, Microstructure, and Wear of Al--10.6Si Laser Surface Alloyed With Additional Silicon, Surface Engineering, Volume 6, 1990.

32. Walker, A.M., Laser Surface Alloying and Cladding of Aluminum Alloys with Silicon, Aluminum Technology, 1986.

VITA

Nathaniel Kennedy was born on April 29, 1975 in Louisville, Kentucky. He is the oldest of three sons born to Bob and Bette Kennedy. Nathaniel graduated from Atherton High School in 1993. In 1997, he received his Bachelor's degree in physics from Eckerd College, in St. Petersburg, Florida. Mr. Kennedy then pursued a Master of Science degree in Engineering Science at the University of Tennessee Space Institute, which he completed in May of 1999. He went on to work for Osram Sylvania in the area of product development.